Potential Future Engine Cycles for Improved Thermal Efficiency

Analysis of Various Internal Waste Heat Recovery Cycles with Minimal Deviation From Common Engine Architectures

MICHAEL J. DENNY

Department of Applied Mechanics
Combustion Division
Chalmers University of Technology
Gothenburg, Sweden 2014

Master's Thesis 2014:32

Potential Future Engine Cycles for Improved Thermal Efficiency
Analysis of Various Internal Waste Heat Recovery Cycles with Minimal Deviation From Common Engine Architectures
MICHAEL J. DENNY

Master's Thesis 2014:32
ISSN 1652-8557
Department of Applied Mechanics
Combustion Division
Chalmers University of Technology
SE-412 96 Göteborg
Sweden
Telephone: + 46 (0)31-772 1000

Thesis performed at:
Volvo Car Corporation
Advanced Engine Engineering Dept. 97624
PO Box PV4B
SE-405 31 Göteborg
Sweden

Printed by:
Chalmers Reposervice
Göteborg, Sweden 2014

Abstract

A comparative 1-D analysis is undertaken between a baseline internal combustion engine (ICE) and several ICE operating cycle concepts which are intended to produce higher brake efficiencies than the baseline which runs on an Otto cycle. The baseline is a spark ignition gasoline engine representative of modern naturally aspirated automotive engines in its architecture and implemented technologies. Engine models are created and compared in the 1-D engine simulation software program GT-Power created by Gamma Technologies. After calibrating the performance of each model with the same resolution and tuning strategies, the result is that all of the concepts are less efficient than the baseline engine. Each engine concept requires additional hardware to separate the processes of the cycle within the engine. These components add to the mechanical friction, flow, and heat losses within the engine, and in some cases manage only to transfer exergy into different forms, not reduce it in a positive way. While the processes of these cycles are intended to improve the brake efficiency of an ICE through internal waste heat recovery or reduction, they first have to overcome the detrimental effects imposed by the architectures they require. This challenge proved too big to overcome and a net decrease in brake efficiency is realized.

Keywords: thermal efficiency, improved thermal efficiency, engine concept, GT-Power, fuel conversion efficiency, future engine cycles, future engines

Acknowledgements

I would like to thank Volvo Cars for sponsoring the thesis, my supervisors Fredrik Ekström and Sören Eriksson and my examiner Ingemar Denbratt for their ideas and critical feedback, Dominik Rether of FKFS for support of the combustion modelling, and the various persons in the support team at Gamma Technologies who proved to be invaluable in helping me construct some of the more difficult engine concepts in GT-Power.

Michael J. Denny

Contents

List of Figures

List of Tables

List of Abbreviations and Symbols

$\eta_{f,b}$	brake fuel conversion efficiency
K	Kelvin
4SRSC	4-Stroke Regenerative Split-Cycle
a	after
b	before
BDC	Bottom Dead Center
BMEP	Brake Mean Effective Pressure
BSFC	Brake Specific Fuel Consumption
CAD	Crank Angle Degrees
CFD	Computational Fluid Dynamics
EGR	Exhaust Gas Recirculation
FMEP	Friction Mean Effective Pressure
HCCI	Homogeneous Charge Compression Ignition
HX	Heat Exchanger
ICE	Internal Combustion Engine
ISFC	Indicated Specific Fuel Consumption
MBT	Maximum Brake Torque
MFB	Mass Fraction Burned

NVH Noise, Vibration, and Harshness

PHEV Plug-in Hybrid Electric Vehicle

SOI Start of Injection

TDC Top Dead Center

VE Volumetric Efficiency

VVT Variable Valve Timing

WOT Wide Open Throttle

1

Introduction

Legislation in 2020 requires that the fleet-average fuel consumption be 40% lower than the 2007 regulations. It is unclear if current gasoline engine technologies such as direct injection, variable valve timing and lift, and strategies such as downsizing and start-stop operation will be able to achieve these future requirements for passenger cars. It follows then, that unconventional engine cycles and architectures may be necessary to achieve the required significant improvement in fuel efficiency.

But why focus on improving the engine? Won't hybridization allow these vehicles to meet these goals? The trivial answer is that even if the requirements can be met with conventional engines in hybrid powertrains, it would consume even less fuel with a more efficient ICE. The non-trivial answer depends on the application, the cost for the consumer and manufacturer, and also on more complex questions not considered here, such as the impact of mining and processing the materials for the batteries vs. drilling for oil or harvesting biofuels. Here these questions are addressed from the perspective of application, cost, and complexity. The application targeted here is long distance driving. On city cycles where total distances are short and there are many acceleration and deceleration phases, PHEV's benefit from reusing the energy recovered during regenerative braking to help accelerate the vehicle again. In long distance (several hundreds of kilometers), near steady state driving, that energy storage will either be saved and not contribute to the tractive force or be drained long before the end of the trip. In this situation the hybrid system only serves to add weight to the vehicle which increases the rolling resistance. From other perspectives it adds more than just weight, it also adds cost for both the consumer and manufacturer as well as complexity. Hybrids have the cost disadvantage of requiring two powertrains. Another drawback is the inevitability of the expiration of the battery pack, which will be a large expense to the consumer. A higher degree of complexity will increase the likelihood of a failure which the manufacturer will see in warranty costs early in the vehicle's life, and the consumer will see as repair costs later in the vehicle's life.

One type of energy recovery system which has shown to be useful for improving steady state efficiency is a bottoming cycle, more commonly referred to as external waste heat recovery. These typically consist of a closed loop Rankine cycle where the working fluid is heated with the engine's cooling and exhaust systems and expanded with a device that takes work from the fluid. The drawback with these systems, however, is that in an automotive application the work they produce is often used to create electrical energy. This obviously requires the vehicle to have a hybrid system, so now it would be composed of three different work producing systems, increasing the vehicle cost and complexity even further. Also, the maximum potential of an external system is below that of an internal waste heat recovery/reduction process. There could be exergy destruction between the ICE and the closed loop system, and the system's efficiency decreases with every number of energy conversion stages in the electrical system from generation, to storage, to output. It may be possible to generate mechanical work directly from the expansion process, but this would incur the efficiency loss of additional transmission components.

Because of these reasons, it would therefore be quite an elegant solution to be able to meet the 2020 legislation without the addition of a second or third powertrain in the same vehicle frame and still benefit from the cost and range advantage of a fairly conventional powertrain operating on non-conventional cycles.

Still, cost remains a concern within this study. The flexibility of the factories where these engines are to be produced must also be considered. For example, the engine block is cast from moulds produced by dies which are very expensive to manufacture, thus a change in the die must be very highly motivated. Likewise, the machining equipment that carry out the final processes can be very resistant to change. A simple change in cylinder bore spacing (which has already changed the casting dies) is not adjusted for at the machining process by the turn of a screw drive as if it were a 3-axis mill. The machines are rigid to maintain high precision, reduce complexity and also wear so the tool spacing is often not adjustable. I was told a story of such a case, based on inside knowledge, in regard to Buick's early V6 engine. The cylinder bank angle was maintained at 90°, the same as the V8 engines, because changing the angle of the machining equipment was too expensive to justify at the time. It also had a crankshaft where cylinders directly across from each other shared crank pins, another V8 attribute. This caused an uneven firing order between the cylinders resulting in poor NVH, but this was deemed as an acceptable compromise. After the V6 architecture proved its value, dedicated manufacturing lines were created for these engines.

Conversely, some components are made from blanks which can remain unchanged in raw form while being manufactured into physically different components with virtually no change in cost. One example here can be cam shafts, provided that the blank lobes are cylindrical. A change in profile may only incur the manufacturing cost of reprogramming the cutting and grinding machines. Therefore, a balance must be found between the expected benefit from a new engine and its deviations from current production.

1.1 Purpose

The purpose of this thesis is to investigate non-conventional engine cycles and architectures which show promise of improving the thermal efficiency of automotive-style gasoline ICEs while avoiding the cost of a completely retooled engine factory.

1.2 Scope

In order to ensure this investigation is limited to a manageable size the following scope is defined:

- Create a baseline engine model in GT-Power, an engine simulation software program, to which the concepts will be compared. The engine should be as representative to a production engine as possible. It and all the concepts will be naturally aspirated.
- Develop models of the concept engines in GT-Power and compare them to the baseline, tracking down the reasoning behind any differences in performance and efficiency.
- The detailed mechanical form will not be created. This means no computer aided solid modelling or multi-dimensional CFD. Only the dimensions necessary for the 1-D analysis the simulation program will perform are developed.
- A detailed analysis of the exhaust gas composition is not considered. Only air-fuel ratios will be targeted and monitored.

This paper is written for an audience of engineers with a thermodynamic and mechanical background who are familiar with power generation cycles and devices including Otto, Diesel, and steam engines. Therefore it is assumed the reader has a certain level of knowledge in these and related topics. Readers not familiar with these subjects should refer to textbooks on thermodynamics and ICE's. The books by Çengel, Heywood, and Moran referenced in the bibliography are suggested. From here on out the efficiency of the engines will not be the thermal efficiency as defined by the ideal gas processes of the engines but the brake fuel conversion efficiency, $\eta_{f,b}$, which is the ratio of the brake power produced to the chemical power of the added fuel, using the lower heating value of the fuel. The fuel used in this study is gasoline.

2

Concept Review

THERE ARE HAVE BEEN, and still are, many claims of technologies which will revolutionize internal combustion engines. Sorting through them to find the ones with true potential can be difficult. Some engines which claim to provide a reduction in fuel consumption have the same fuel conversion efficiency of a conventional engine. Some examples are the cam-style engines discussed later. The difference is that they have various clever ways of packaging the engine's components which increase the power density in terms of mass. The fuel reductions they claim then are gained in urban driving cycles and are a result of the change of energy required to accelerate a lighter vehicle at the same rate. The steady state fuel consumption will remain unaffected with these engines (since the mass difference is on the order of tens of kilograms, the difference in the absolute value of rolling resistance will be small). The goal is to identify and evaluate designs whose characteristics reduce the thermal losses from an engine. This energy is most notably lost to the cooling and exhaust systems as well as the mechanical friction, or perhaps more properly described as viscous dissipation due to the nature of most "contact" joints in engines.

2.1 History's Lessons

Previous engine architectures which are no longer around may have failed for reasons which are easily remedied today, had their funding pulled, or maybe were just unpopular at the time and were simply forgotten about. Therefore it is possible that a good engine design from the past could be applicable today.

2.1.1 Compound Engines

In the late 19$^{\text{th}}$ and early 20$^{\text{th}}$ centuries there were several physical examples, as well as some designs and patents that did not make it to fruition, which focused on compound expansion to decrease the exergy of the exhaust gases. Compound expansion means that the expansion process is broken up into a series of stages. For internal combustion engines two stages were typically used. Compound expansion showed up earlier in steam engines to improve their efficiency, and then three or more stages were often used. The reason for the increase in efficiency was due to the lower temperature fluctuation in any given cylinder. If complete expansion was to take place in a single cylinder, the heat flux of that cylinder would be higher. Every transition from a high temperature to a low temperature is irreversible (unless work is added). Therefore, a smaller difference in temperature between the faces inside the cylinder after the exhaust stroke and the hot incoming steam meant less heat lost to the structure of the engine.[2]

With ICE's, however, the main advantage comes from obtaining complete expansion of the exhaust gases in the first place. Recalling an ideal Otto cycle, the expanded pressure and temperature is not equal to that at the start of the compression stroke. In order for complete expansion of the combustion products to be achieved, the expansion ratio needs to be greater than the compression ratio. In this sense a compound internal combustion engine is similar in thermodynamic operation to an ideal Atkinson cycle.

The early compound engines were large stationary engines. Most of them had an inline three cylinder configuration with the two outer cylinders firing on a four stroke cycle and the center cylinder operating (but not firing) on a two-stroke cycle. The center cylinder is, among the engines studied, unanimously of larger bore and 180° out of phase of the two in-phase outer cylinders. The outer cylinders fire 360° apart and alternately transfer their exhaust gasses to the center cylinder where they are expanded further. The firing and expansion cylinders are connected via a port with valves and this creates a pressure drop between them during the gas transfer. Therefore, additional work is gained from the additional force in the expansion cylinder due to the difference in bore area between the two. Some examples also exhibited a longer stroke for the expansion cylinder which also would have provided a torque advantage from the difference in crank throw radii, albeit continuously varying throughout every revolution.

One failed example of this kind of engine has firing cylinders operating on the Diesel cycle, was constructed in 1897 and actually comes from Rudolf Diesel himself. A partial drawing can be seen in Figure 2.1. Instead of being more efficient than a typical diesel engine it was actually half as efficient and only achieved two-thirds of its targeted power output of 150 *hp*. Investigations were made into why the efficiency was so low and it was discovered that the four water cooled valves, labelled "A," in Figure 2.1 absorbed a significant amount of energy as did the transfer ports which also induced pumping losses. One can speculate that having six piston rings on the low pressure expansion cylinder is overkill and unnecessarily added to the friction losses in the engine. The expansion piston was cooled internally with some liquid and that too would have been a significant source of exergy loss. After taking three years to build the engine, its performance was so disappointing that it was run for only three months before it was dismantled and scrapped.[1]

Wihin the following decade, in 1904, Edward Butler created three examples of his stationary compound engine which, he claims, produced positive power from the expansion cylinder when running on oil. The overall engine layout was similar to that of

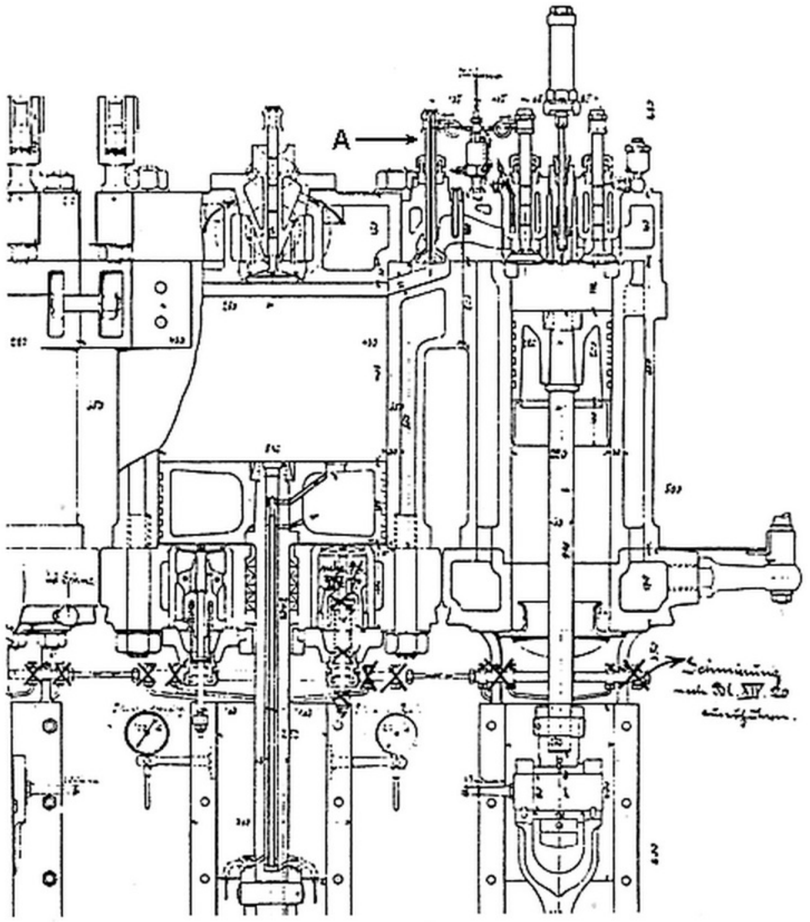

Figure 2.1: Parital drawing of Rudolf Diesel's compound engine. From *The Diesel Engine*, Cummings, p185.

Diesel's design, but there are no detailed drawings to present. Total power output of the engine was 80 *hp*, and 20 *hp* was said to be produced by the expansion cylinder.[1] Fifty percent of the firing cylinder's BMEP seems quite high as does the 25% increase in $\eta_{f,b}$. Unfortunately no independent measurements are mentioned. A more likely story is that of the Duetz engine from 1879. Like the Diesel-compound, it too suffered from high thermal losses to cooled transfer valves and the expansion cylinder barely generated enough power to cancel out its own friction.[1]

2.1.2 Cam and Axial Engines

Cam engines are different from axial engines in this context in the way that the pistons transfer their force to the output shaft. They are similar in their flexibility of cylinder arrangement and therefore power density in terms of mass. They all run on conventional engine cycles, however. They are mentioned here briefly because it is in this flexible arrangement that they are able to have different instantaneous torque profiles compared to crankshaft engines. In some cases, piston side-forces can be cancelled out which is attractive for reducing friction, but often comes at the expense of increased complexity and inertia (i.e. the addition of roller bearings).

Cam engines tend to have a flat profile with their cylinders arranged radially in a plane. The pistons ride on a symmetric cam profile, often with roller bearings. The linkage can take many forms, but one example called the Fairchild-Caminez Cam Engine from 1926 is pictured in Figure 2.2a. Axial engines have their cylinders arranged parallel to each other and the output shaft (sometimes the engine block is the take-off point). The cylinders are arranged in a circular pattern and therefore cylinder counts above three occupy nearly the same amount of space. This is due to the diameter of the wobble or swash plate that the cylinders ride on. To avoid extreme angles to get the same amount of cylinder stroke the cylinders must have adequate spacing from the engine's axis. One example of an axial engine is the Macomber Axial Engine from 1911 pictured in Figure 2.2b. Axial engines were actually quite popular in the early 20$^{\text{th}}$ century as airplane engines and showed up on several models.[1]

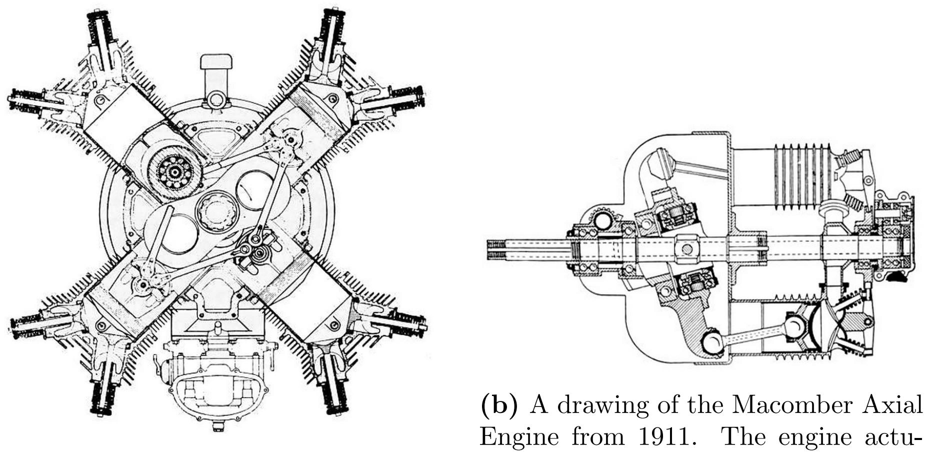

(a) A drawing of the Fairchild-Caminez Cam Engine from 1926.[1]

(b) A drawing of the Macomber Axial Engine from 1911. The engine actually has 7 pistons arranged in a circular pattern.[1]

Figure 2.2: Examples of cam and axial engines.

2.1.3 Combined Cycle

An engine called the Still Steam-Diesel Engine (named after its creator, William Joseph Still) from 1924 was the most efficient of the historical engines studied. It was proven on several seafaring ships and locomotives where both its performance and efficiency were measured. The engine operates on a combination of parallel Diesel and Rankine cycles. The latter received its energy in-part from the head and cylinder liner of the engine and external waste heat recovered from the exergy in the Diesel exhaust. The remaining portion came from a conventional boiler. This heat recovery was key to the engine's high efficiency of 41% (all fuel sources). This compares to a maximum Diesel engine efficiency of 36% and steam turbine efficiency of 20% for that era, according to an article from Captain Frank Acland in 1920.[3] The first expansion process of the Rankine cycle acted on the bottom side of the Diesel piston. Any left over steam exergy after the piston expansion went on to power a small turbine which was connected via a shaft to an air compressor for the Diesel side of the engine, and generate electricity if there was still enough exergy in the steam to do so. The electric generator would act as a motor for the compressor when the steam could not power the turbine. This type of engine arrangement can be seen in Figure 2.3. It was most efficient in its second form, powering

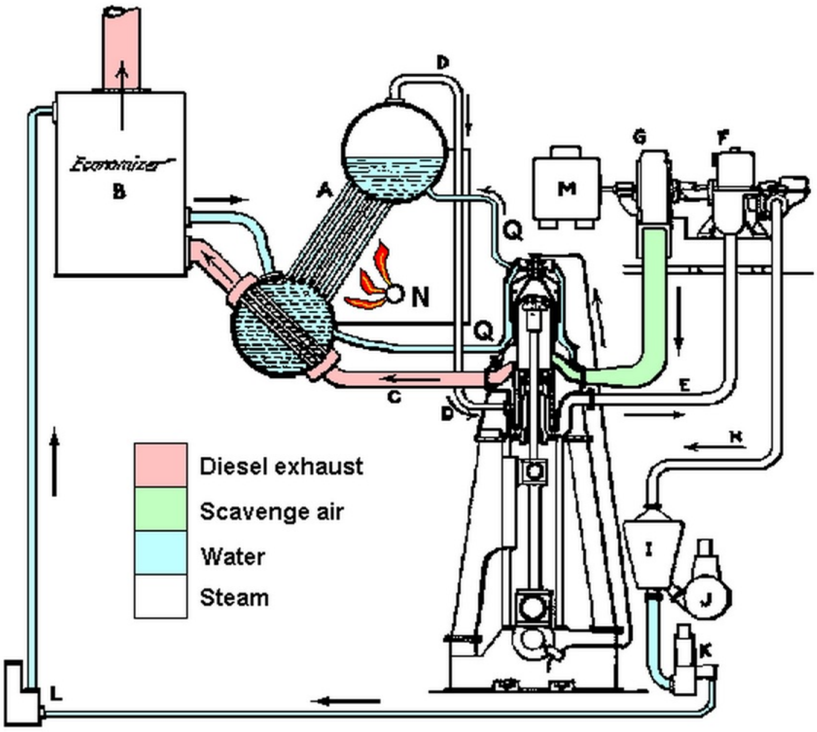

Figure 2.3: Functional diagram of the Still-Diesel Engine.[1]

the cargo liner *Eurybates*, where instead of all the cylinders having double acting pistons, four cylinders operated on the Diesel cycle, and two cylinders were used for the steam expansion. This eliminated two problems, both related to contamination. The oil from the cylinder liner would no longer mix with the steam and contaminate the boiler, which reduces its efficiency, and the steam would no longer contaminate the lubricating oil for the Diesel engine, which reduces its lubricity.

One reason its popularity did not catch on, despite its high efficiency, was apparently due to a lack of workforce specialization. These engines required the ships to have Senior Engineering Officers who were qualified for both steam power units as well as Diesel engines. Apparently at the time, people with both these qualifications were drawn more towards jobs located on land.[1] Another drawback of this engine, and as we will see, many engines which have methods to increase the fuel conversion efficiency, will have a lower power density in terms of total cylinder volume than their standard versions. Later in the ship's life in 1948, efficiency was traded for power and the two steam cylinders were converted into Diesel cylinders.

2.1.4 Regeneration

The Stirling engine is a very well known example of incorporating regeneration, the act of storing heat from a heat rejection process in the current cycle to use it in a heat addition process during the next cycle. This increases the efficiency of the engine because less heat is rejected to the atmosphere. There are drawbacks to regeneration in practice, however. The first is a problem of time. Due to the fact that the mass which will be absorbing and releasing the heat energy cannot change temperature instantaneously, a reduction in time between cycles also correlates to a reduction in the regenerator's effectiveness (ability to absorb and release all the heat energy possible). This limits the maximum engine speed where high efficiencies can still be reached. Another detriment is the structure of the regenerator itself. If it is to transfer heat quickly, it must have a very high surface area. In a limited volume, this means that the flow areas within the regenerator will be very small. Steel wool is one example of what the regenerator is sometimes made of, and this or any similar substrate with a very high surface area to volume ratio adds significantly to the pumping work of the engine.

The Ericsson engine is similar to a Stirling engine with the differences being the constant volume processes are instead constant pressure processes and the Ericsson engine runs on an open cycle. Their connection to the Carnot cycle is they all share the same ideal efficiency. Both the Stirling and Ericsson engines get their heat through external combustion which means that the transient response will be on the order of seconds (or more for very large examples) due to the cylinder's heat capacity. An internal combustion engine has a massive advantage in this respect as load can be varied from one cycle to the next. Another disadvantage of these two engines is their low specific output in terms of both volume and mass. It's clear that these engines are not well suited for personal vehicle applications but the take-away is understanding why they are efficient. The recycling of heat is the main cause for their efficiency, but as stated earlier, carrying out this process quickly is countered by reduced regenerator effectiveness and higher flow losses.

2.2 Today's Ambitions

Not seeing any directly applicable concept or example from the past for today's vehicles, the search continues. There are several engine concepts which have been created in the last couple decades which aim to improve the efficiency of ICE's. Some remember the triumphs of the past and try to incorporate their processes in a modern package.

2.2.1 Idealizing the Otto Cycle

In practice, it is not possible to have a truly constant-volume (isochoric) heat addition in an ICE. As a result, the sharp corners at the end of the compression stroke and beginning of the expansion stroke of an ideal Otto cycle P-v diagram end up becoming fillets, reducing the indicated work of the engine. Therefore, it logically follows that creating a mechanical linkage which allows the cylinder volume to remain nearly constant during the finite combustion duration would generate a more ideal engine cycle in practice. Masatoshi Suzuki (from Honda Motor Corp.) et al. investigated this possibility. But first, a quick review of instantaneous piston velocity. Since the piston in a typical engine is not directly pinned to the crankshaft and the connecting rod used to join the two is not of infinite length, the piston's velocity is not sinusoidal. The piston's speed is higher during the upper 180° of motion and lower during the bottom 180° compared to a true sine wave. So, taking advantage of this knowledge, Suzuki et al. arranged an engine where the crankshaft was above the combustion chamber and two connecting rods reached down, one on either "side" of the cylinder, to connect to the bottom end of the piston. By doing this, the piston now exhibited a velocity profile around TDC identical to what normally occurs around BDC. While this still does not provide an absolutely isochoric heat addition, it gives insight into the trend the actual pressure trace takes the nearer it gets to an isochoric process.

What they discovered is that despite an increase of 15% in maximum cylinder pressure, ISFC increased by 5% compared to the base engine. Shortly after the spike, the in-cylinder pressure trace falls slightly below that of the base engine for the remainder of the expansion stroke. They found that the reason for this was due to increased heat losses to the combustion chamber walls. The increased dwell time of the gases at their hottest point during the period where the surface area to volume ratios are their highest were more detrimental to the efficiency than the increased peak pressure was beneficial.[4] As a visual aid to help appreciate this phenomenon, the fluctuation in the ratio of cylinder surface area vs. volume over a four-stroke cycle with a compression ratio of 12.5:1 is shown in Figure 2.4. Not only is the magnitude of the ratio at TDC over 7 times that occurring at BDC, but the upper 84% of that fluctuation occurs in just the first quarter revolution before and after TDC - the portions of the stroke that Suzuki had slowed down. Trying a different strategy, they created engines with a conventional piston-crankshaft placement but with high connecting rod length to crank radius ratios. This still causes the piston speed near TDC to be faster than a true sine wave, but closer to it with higher and higher ratios. For homogeneous charge combustion they found the same trend; a drop in fuel conversion efficiency. However, with stratified charge combustion they saw a 1% improvement between the connecting rod length to crank radius ratio of 3.34:1 and 8:1. They attributed this to the insulating properties of the air surrounding the combustion and the slow flame speed near the lean regions of the mixture. A side benefit they discovered as a part of this investigation is that for homogeneous charges, faster piston speeds near TDC lower the propensity for knock since a larger volume near the end of combustion means lower pressures and temperatures.[4]

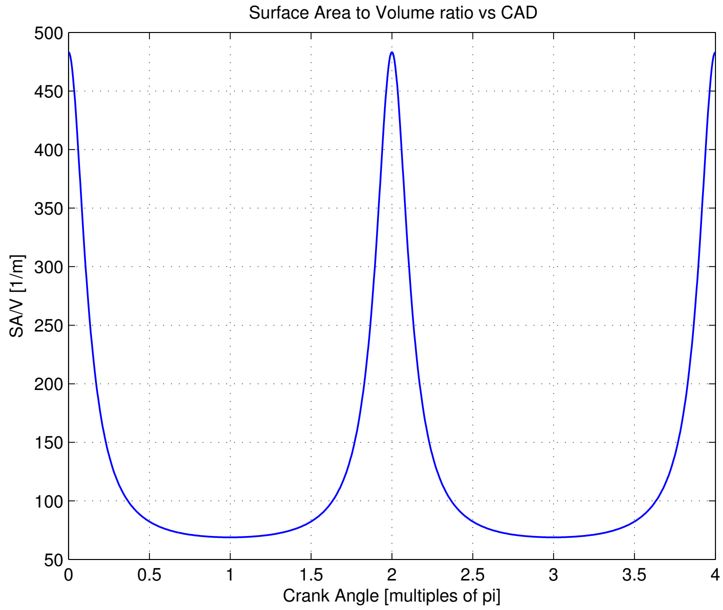

Figure 2.4: Fluctuation in the ratio of cylinder surface area to volume over a four-stroke cycle with a compression ratio of 12.5:1 with 5 mm of clearance at TDC. TDC first occurs at 0 multiples of pi.

2.2.2 Differential-Stroke Cycle

Yan Engines is a relatively new company that moved into the U.S.A. in 2011 which is developing an engine that they call the Differential-stroke cycle, or D-cycle for short. Unfortunately, the experimental results of this engine have not been published as of writing this. Their claimed fuel consumption reduction is a quite literally unbelievable 80% compared to that of a normal diesel engine. They also claim a 100% increase in torque and power based on displaced volume. This is becuase the engine has two power strokes per revolution. There must be some sort of validity to their claims as they have have won funding through the United States Department of Defense three times over with the amount of money granted increasing at each stage. To date, they have been awarded a total of $4 million. Their aim is for this technology to be retrofitted into heavy duty diesel engines - the staple of the powerplants for the U.S. Military.

A brief theory of operation of the engine is such: A piston is split into two parts, upper and lower. The lower portion is connected to a connecting rod and exhibits normal piston motion. The top portion is connected via a linkage to a so called pistontrain, similar to a valvetrain in that it has cams and rocker linkages. Via spring force, the top portion of the piston is biased to sit at the top of the combustion chamber and is pushed downward with the cam to alter its position. During the compression and power strokes, the two portions ride together in contact. Near the end of the power stroke, however, the exhaust valves open, the cam allows the spring to push the top portion back up to the top of the cylinder, exhausting the gases. The exhaust valves close, the intake valves open, and the piston's cam then pushes the top portion back down and air is drawn into the cylinder. After this process the piston portions meet back up for the compression process. The piston splits apart for roughly 140° centered around what is BDC for the lower portion of the piston. Some things they point out is that with the same stroke the displaced volume is decreased, but can be compensated for with supercharging in some way. They also point out that the same technologies applied to valvetrains such as variable timing and lift can be applied to the pistontrain as well.[5]

Some drawbacks to this engine architecture are mostly due to its kinematics, and it is clear why whey are focusing on low speed heavy duty diesel engines. Since the actuating rod for the top portion of the piston runs through the center of a split connecting rod that supports the bottom end of the piston there are a lot of stress concentrations in both which do not lend themselves to durability at high mean piston speeds. On that same subject, the maximum mean piston speed for the engine is that of the top portion during the gas exchange process. The top portion's acceleration at TDC is just countered by a slender rod as opposed to the entire connecting rod. It also seems like the efficiency for this engine would decrease at high loads where the blowdown pressure may be significantly higher than in a conventional 4-stroke engine. This would be due to the lower expansion ratio for the same crank radius.

2.2.3 Revetec

This engine was on the verge of omission since it still operates on a typical Otto cycle and just appeared to be another method for increasing power density. What earned its recognition here, however, is its measured maximum $\eta_{f,b}$ of 39.5%. The engine has opposed pistons which are connected to each other and have separate combustion chambers on opposing sides of the engine. Using roller bearings, they ride on two co-axial tri-lobe cams located between the pistons which actuate in a scissoring pattern as they counter-rotate. This eliminates piston side-forces but puts a twisting moment in the connecting structure that joins the pistons. These cams are geared to the output shaft and are the means by which the engine turns cylinder pressure into rotational motion.

Recall what was discussed earlier about isochoric heat addition. In slowing the piston down near TDC, the peak pressure was increased, but the mean pressure was decreased due to the higher degree of heat transfer. With a cam engine, the piston's velocity is free to be altered at any point in the cycle. It would be possible to truly stop the piston for some duration at TDC, and allow it to quickly accelerate downward after combustion had at least mostly been completed. Remember, the piston's velocity in Suzuki's engine was slower during the first 90° of the expansion stroke, a significant duration. Have Revetec achieved a more favorable piston motion with the cam? Without knowing the cam profiles, it is not possible to say for sure. It may be that the only advantage their engine has over a conventional one is the reduced friction through fewer journal bearings and elimination of the piston side-forces.

2.2.4 Over-Expansion Cycle

As you'll recall from before, the compound engines of days past were either less efficient than their standard competitors, or at best, equally efficient but less power dense. A new take on this concept has given it new potential, however. The first change is to maintain a common cylinder bore. This allows the engine block to remain unchanged. The engines would still have adjacent cylinders in multiples of three, which mean inline three or inline and "V" six cylinder arrangements would be the most common layouts. This concept has been named the Over-Expansion engine not because it is intended to expand the exhaust gases below atmospheric pressure but because the expansion ratio is larger than the compression ratio.

Using Figure 2.5 as a visual aid, this engine operates as follows: The outer two cylinders have their intake processes 360° apart and alternately share expanding combustion gases with the center cylinder whose piston reciprocates in-phase with those in the outer cylinders (all pistons would move together). The combustion takes place in a chamber between the outer and inner cylinders. Intake air is compressed into this chamber, and a valve connecting it to the center cylinder opens at the start of the combustion process. The combusted gases then expand into both cylinders where the effective piston area and expansion ratio would be twice that of the compression process. Exhaust valves in both cylinders open to release the exhaust gases on the following upward stroke. The center cylinder then aids in the expansion process from the other cylinder on the next stroke. One potential issue may be heat build up in the center piston since it is only exposed to hot combustion and exhaust gases. Compared to a standard gasoline engine, the overall architecture is identical. The only significant differences are the phasing of the crank throws and port arrangement in the head.

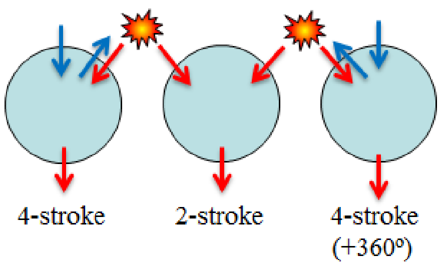

Figure 2.5: Simplified representation of the Over-Expansion concept. The circles represent the cylinders and the arrows represent the direction of the airflow through the engine. Blue is intake air and red is combustion and exhaust.

2.2.5 Recombustion Cycle

This next engine concept combines HCCI and Stratified charge combustion processes not only into the same engine, but also acting on the same air-mass in series. One of the benefits this concept has is stoichiometric exhaust products, which are not the result of these combustion methods individually. This allows for the use of a conventional three-way catalyst and does not require an additional NOx trap typically necessary for lean burning engines. This stoichiometric mixture is achieved by running the first combustion processes at a lambda value of 2, and the second at a lambda value of 1. This sequence burns 50% of the inducted air during each combustion process with an EGR portion of 50% in the second. This does mean that the engine would have to be throttled to vary the load. This engine type has multiples of two adjacent cylinders therefore any existing block with an even number of cylinders could be used.

Using Figure 2.6 as a visual aid, the series of processes for this cycle are as follows: Each cylinder operates on a four-stroke cycle. Air is drawn in, compressed, ignited, and expanded as usual with stratified charge combustion. The adjacent piston is 180° out of phase and its intake stroke is simultaneous with the first piston's exhaust stroke. The cylinders are connected via a port, likely closed off with poppet valves. The architecture still allows for a four-valve head. Having been transferred with some volumetric efficiency, the gases are compressed, ignited, expanded, and exhausted as in normal HCCI operation.

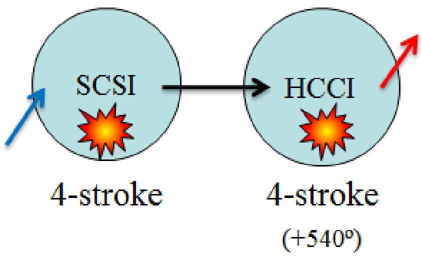

Figure 2.6: Simplified representation of the Recombustion concept. The circles represent the cylinders and the arrows represent the direction of the airflow through the engine. Blue is intake air, black is the transferred air, and red is exhaust.

Despite being susceptible to throttling losses, these combustion processes can still provide thermodynamic benefits when compared to a homogeneous charge spark ignition combustion process. The stratified charge combustion process exhibits reduced thermal losses. The air surrounding the combustion insulates the hottest gases from the cylinder walls and reduces the thermal loss to the coolant system. In the following process, the very high burn rate of HCCI combustion (approximately four times as quick as flame-front propagating combustion) creates a near isochoric heat addition process with typical piston velocities, creating a P-v trace nearer that of an ideal Otto cycle.

2.2.6 4-Stroke Regenerative Split-Cycle

The 4-stroke regenerative split-cycle engine incorporates a regenerative process by where the exhaust gasses heat the intake gasses but through a divided heat exchanger. This engine requires a minimum of two pistons, but it is most likely that this engine would require multiples of three cylinders.

Using Figure 2.7 as a visual aid, the theory of operation for this engine is as follows: Air is drawn into a compression piston cylinder which operates on a two-stroke cycle.

The displacement of this piston is dependent on the number of firing piston cylinders it feeds. It should have half the swept volume of the firing cylinder if there is a one-to-one pairing and the same swept volume if there is a one-to-two combination. The intake air is compressed into the colder side of a heat exchanger connected to the cylinder where it is heated. A separate firing cylinder connected to the opposite end of the cold side of the HX operates on an Otto cycle. It draws-in this heated air during its intake stroke. Somewhere during the intake and/or compression stroke fuel is injected, with the intent that a homogeneous charge is created. The mixture is compressed and ignited by a spark and the power stroke follows. The exhaust stroke evacuates the firing cylinder from the exhaust gases which pass through the hot side of the HX and then into the atmosphere. The cycle then repeats. The intent of the HX is to reduce the compression work by building pressure by heating the intake charge.[6]

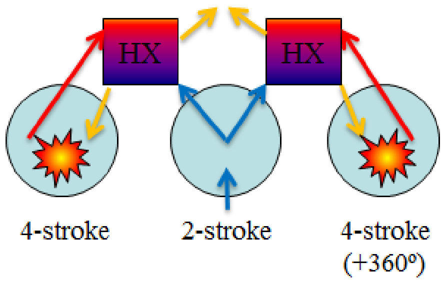

Figure 2.7: Simplified representation of the 4SRSC concept. The circles represent the cylinders, the boxes labelled HX represent the heat exchangers, and the arrows represent the direction of the airflow through the engine. Blue is intake air, orange is heated intake and cooled exhaust, and red is exhaust.

2.2.7 2-Stroke Regenerative Split-Cycle

The 2-stroke regenerative split-cycle concept is a combination of several of the above concepts. It incorporates the strategies of regeneration and over-expansion. This engine type has multiples of two adjacent cylinders therefore any existing block with an even number of cylinders could be used. It has a regenerator which heats the incoming air to reduce the compression work, and has an expansion cylinder which is separate from the compression cylinder which further allows the expansion ratio to be greater than the compression ratio. This can allow for complete expansion of the combustion products.

Using Figure 2.8 as a visual aid, this engine operates with nearly identical processes to the 4-stroke regenerative split-cycle concept with the following deviations: The HX volume for the intake charge is much smaller and is likely realized as a transfer port contained within the head of the engine with some means to transfer the exhaust energy to the intake charge. Both cylinders operate on a two-stroke cycle. The two pistons are phased 180° apart from one another. With this phasing the compressed air will spend a mean time of slightly more than 180° in the HX connecting the two cylinders before it is drawn into the firing cylinder. The intake process into the firing cylinder must happen quickly since this process can only begin after the exhaust valve is effectively closed. If not, the compressed and heated intake mixture will short circuit through the firing cylinder. Unless high amounts of EGR are desired, this means the intake process can only start after TDC, and that combustion can only start after the transfer valve has closed since expanding into the port volume causes a reduction in work. This pushes the 50% burn point late in the expansion stroke compared to a standard engine. The intent is that in the end the reduced compression work combined with the difference between the compression and expansion ratio will overcome the greatly reduced peak cylinder pressure as a result of combusting the mixture so late in the expansion stroke.

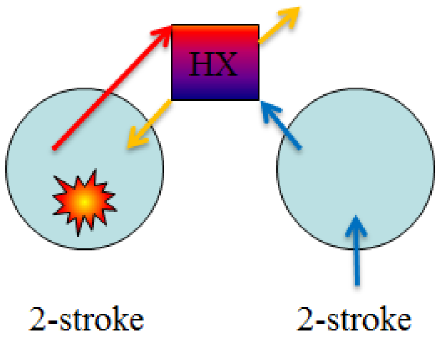

Figure 2.8: Simplified representation of the 2SRSC concept. The circles represent the cylinders, the box labelled HX represents the heat exchanger, and the arrows represent the direction of the airflow through the engine. Blue is intake air, orange is heated intake and cooled exhaust, and red is exhaust.

2.2.8 6-Stroke Otto-Steam

The final modern concept runs on an Otto cycle followed by a steam expansion and exhaust stroke, hence its name, 6-Stroke Otto-Steam. In less developed variants, unheated water can be injected into the cylinder with the hope it will vaporize and expand. This method only reduces the cooling system's exergy as it will obtain the heat energy only from the components in the cylinder. In more advanced variants, the water would be preheated, reducing the exergy of the cooling and exhaust systems. The first preheating stage would take energy from the cooling system, then from the higher temperature exhaust system. If necessary, a heating element could add additional energy when the exhaust exergy is insufficient to reach the desired water temperature. The exhausted steam could be released to the atmosphere, where the cycle couldn't really be called an open Rankine cycle since there would be no condenser. If the steam were captured in a closed loop system, however, the overall cycle becomes a combination of an Otto and Rankine cycle in parallel, with their expansion and exhaust processes occurring in series (it should be noted the exhaust process isn't an official process of the Rankine cycle, but still required in practical applications as there is some distance between the expander and condenser).

There have been several theoretical investigations into this concept, and one physical prototype. The prototype was created by Bruce Crower, the owner of Crower Cams & Equipment Co., Inc. It was run, but not tested on a dynamometer as of 2006, which is also the latest date information can be found for this project. He had modified a single cylinder Diesel engine by using the fuel injector as the water injector. The engine was carbureted and ran on gasoline fuel. The cams were run at a speed of 3:1, as is necessary with a six-stroke engine, but the exhaust cam had two lobes on it which opened the exhaust valve at the proper times. His claims were a 40% reduction in fuel consumption and the ability to eliminate the need for a cooling system, but these are unsubstantiated. It is not clear if all of the exhaust gases were evacuated from the cylinder before the steam expansion stroke.[7]

One of the theoretical studies done through calculation and engine simulation was done by James Conklin and James Szybist of the Oak Ridge National Laboratory. Fearing that repeated thermal shocks to the hot surfaces of the combustion chamber may cause cracks over time with liquid water impingement, they focused on using the energy from recompressed exhaust gases to supply the heat energy for water vaporization. Their assumptions were that the water injection, vaporization, and homogeneity occur instantaneously and that there was no heat transfer from the walls to steam mixture. A minimum cylinder pressure of 1 bar absolute and minimum mixture temperature equal to the saturation temperature of the steam were limits for the conditions at the end of the steam expansion stroke. This was to avoid negative work from sub-atmospheric pressure and to avoid condensation buildup in the cylinder. They found that due to the work required to recompress hot exhaust gases, the most efficient results were found when only a portion of the exhaust was recompressed. Since they only used the cooling system's exergy to heat the injected water, a temperature of only 100°C was achieved. Without pumping or friction losses, the maximum IMEP they were able to achieve from the exhaust compression and steam expansion process was 2.5 bar, or a 25% increase over just the Otto cycle. This would represent a 25% reduction in indicated fuel consumption. They noted in the conclusions that had the injected water temperature been raised to 175°C, the IMEP of the steam process could be raised by 40% to 3.5 bar. [8]

Another study on the potential of this concept was conducted by Bernard Johnson and Chris Edwards of Stanford University. It went away from the six-stroke convention but retained the idea of combining the Otto and Rankine cycles. In this variation the engine operates on an Otto cycle with the steam expansion and exhaust strokes occurring simultaneously with those of the Otto cycle. The steam is injected during the combustion process. They had also incorporated low heat rejection strategies to reduce the thermal losses to the cooling system. However, focusing just on the gains from the steam expansion process they found a 4.7% improvement in efficiency after they had imposed a 5% combustion efficiency penalty since steam is injected during the combustion process. This penalty is unmotivated, however. This is a relatively small improvement in efficiency, but it is on top of the improvements gained through the high compression ratio of 17:1 they assumed could be feasible and a low heat rejection cylinder.[9]

2.3 Selected Concepts

The concepts which will be studied in detail are the:

- Over-Expansion Engine
- Recombustion Engine
- 4-Stroke Regenerative Split-Cycle Engine
- 2-Stroke Regenerative Split-Cycle Engine
- 6-Stroke Otto-Steam Engine

I must state that I did not create these concepts myself. They were either presented to me for investigation, discovered through research, or developed jointly through discussion with other powertrain engineers.

3

Method

In order to create a fair comparison between the different concepts, several characteristics are kept constant between them. Operating limits in the mechanics and thermodynamics of the concepts are also imposed with practical limits in mind so that they are representative of what could be achieved in a physical representation. The engine concepts will be compared to a baseline engine which is also created in GT-Power and adheres to the same limits. This minimizes the possibility for misleading results and conclusions to be drawn from the simulated performance of the concepts.

3.1 Simulation

Since ideal cycles are well understood in the engineering community and the results they predict are very dependent on the assumptions made in their calculation, a more accurate, predictive method of analysis is used to obtain results. This provides a more realistic approximation of the performance these engine concepts would exhibit in physical form.

In order to achieve this, the software package GT-Power by Gamma Technologies is used for all engine performance calculations. The predictive combustion model created by the Forschungsinstitut für Kraftfahrwesen und Fahrzeugmotoren, Stuttgart aka FKFS (translates in English to the Research Institute of Automotive Engineering and Vehicle Engines, Stuttgart) is an add-on to GT-Power and is the default method used to calculate the combustion process. The exception is in cases where the intended combustion process is outside the capabilities of the model. In these situations the combustion process is modelled based on the works of various researchers who were able to draw conclusions from physical testing. More information on how combustion was modelled in those cases will be covered in their respective sections. While GT-Power has the capability to incorporate multi-dimensional flows, in these analyses it is used as a 1-D engine simulation program. Taking advantage of its multi-dimensional capabilities requires creating detailed 3-D models of the engines to be studied and is far beyond the scope of this thesis and not even something pursued extensively in the industry. In practice, identical or similar component testing is performed along with separate 3-D CFD simulations and the characteristics of these 1-D components and mechanical models are scaled to match the results of the more detailed analyses. By this measure, there is minimal loss in accuracy by using a calibrated 1-D simulation program. This is, infact, the method by which several models that calculate the performance of the studied concepts are developed.

3.1.1 GT-Power

For those unfamiliar with GT-Power, a brief description of what this program is used for, and why, in the scope of this thesis is provided here. GT-Power is a specialized type of CFD program which solves the compressible Navier-Stokes equation in one dimension. It calculates an array of properties of the working fluid (typically air) and has built-in calculations to provide common metrics by which the user can analyze the performance of the engine or subsystem. The user is also free to add equations to the simulation to provide other metrics. The user constructs the layout of the gas exchange system by connecting a series of pipe, volume, and valve elements to represent the intake and exhaust systems connected to cylinder elements by defining diameters, lengths, etc. It calculates the properties at CAD intervals within one complete engine cycle. The CAD intervals are based off of the current engine speed and time intervals determined by the time it takes for a pressure wave to travel the distance of the characteristic length set by the user. There are other factors in this equation, but the strongest correlation is to the speed of sound. Since they suggest that the characteristic length be set at approximately 40% of the bore diameter, at low engine speeds the CAD interval is very short - a fraction of 1° - and there can be thousands of time steps for even a two-stroke cycle. At maximum engine speed, however, the intervals are on the order of 3-4° which significantly reduces the simulation time for a cycle. The results from one cycle are used as inital values for the next and the solver continues to iterate through complete cycles until the convergence criteria are met. The properties in the different flow elements at each interval can be displayed as instantaneous values throughout the cycle or integrated over the cycle for a single value. For example, the user can view the pressure trace from the cylinder, or the IMEP for the cycle, respectively.[10]

The strongest benefit this program provides over even the most detailed hand calculations is capturing the impact on volumetric efficiency from pulsatile flow, the flow losses caused by the geometries of the engine (valves, orifices, flow areas, wall friction, etc), the heat transfer between the gases and engine components, and the friction in the engine (usually modelled, not calculated). With the FKFS model add-on, the benefit is that an assumed burn duration (i.e. Wiebe curve) can be replaced with a predictive combustion calculation. If enough testing has been done on a similar engine to calibrate a base model with, there are enough input parameters available that almost nothing about the engine's operation has to be assumed, and this is what makes it such a valuable tool for engine engineers; to understand how even just changing one characteristic affects the various performance metrics of an engine.

3.1.2 FKFS Cylinder Object

The FKFS cylinder object provides several benefits to the end user which greatly reduce the amount of control parameters the end user needs to impose in order to simulate a properly running engine. The first is its ability to phase combustion automatically to avoid knock. In-cylinder turbulence coefficients and knock limit coefficients are first found through CFD and/or experimentation. By using these, the dwell time of the fuel in the air, its temperature, and other factors, it predicts the onset of knock based off of the Worret knock model. If the calculated values are above the set knock limits it retards the desired mass fraction burned anchor (in this case 50% MFB) in steps until the probability of knock is below the limit. It does this within the same cycle that GT-Power is calculating. The other benefit it provides is calculating the burn duration, which varies with load and speed, which the user otherwise has no good motivation for defining other than through experimentation.

If the cylinder object did not do this, the engine load map would have to be generated, knock probabilities checked, and MFB anchors phased to values assumed to be correct, and iteratively run through this process. The optimizer in GT-Power can also be used to find these values, but it also a very lengthy process due to the simulation time. Then, if any parameter is changed and it affects the volumetric efficiency or gas temperatures, the process needs to be repeated to ensure knock does not occur. This process easily adds hours of simulation time and it is still without the benefit of calculated combustion duration.

FKFS created and verified their model by comparing its results to experimental data gathered from several different engines.[11]

3.2 Model Standards

In order to provide a fair and accurate comparison, several model standards were set both on the operational and geometric characteristics of the engine. A selection of those with the greatest impact can be seen in Table 3.1. There are also some characteristics which are better stated than listed.

3.2.1 Flow

In general for the flow components, the diameters are always rounded to the next largest whole mm if the calculated value is more than 0.1 mm over. The motivation behind this rounding is that pipes are typically manufactured at whole number intervals. The exception to this is for partially out of phase flow splits where the expansion diameter no longer has a strong physical meaning. Flow splits are special cases in that respect since the diameters that define them are used to calculate a flow area rather than a physical diameter. For example, if a “Y” flow split has a flow direction from the branches to the single outlet and the flow in each branch occurs simultaneously (in-phase) the area one branch can effectively “expand” into is half the actual area of the outlet. If the flows are completely out of phase, the expansion diameter would be the full physical diameter of the single outlet.[10] For this reason, rounding can no longer be motivated for out-of-phase flow split diameters.

The displaced volume of the engines is an important point to specify since normal conventions no longer apply. It is no longer based on all of the cylinders in the engine. The displaced volume of these engines is defined as the total swept cylinder volume of all intake strokes from the atmosphere in one cycle. This means that for engine concepts which transfer the gases from one cylinder to the next, only the displaced volume of the cylinder that took the air from the atmosphere counts. This still lies in convention with normal Otto cycle engines. In these concepts the device which takes work from the gases a second time just happens to be a piston cylinder. If it were a turbine with a shaft providing mechanical work, it becomes clear that trying to add a displaced volume for the second expansion device has no meaning as the flow into it is based on the displaced volume of the cylinder taking air from the atmosphere.

3.2.2 Cylinder

Concepts allowing the use of FKFS cylinder objects all had identical values for the in-cylinder turbulence coefficients and knock targets. This is due to the fact that these values either have to be experimentally measured or predicted with three dimensional CFD. Refinement of combustion chamber, port, and valve geometries is extremely resource intensive in terms of manpower, simulation methods, and simulation time. For this reason, in all respects other than compression ratio, the characteristics remain identical between the engines using the FKFS cylinder object. In special cases, the compression ratio was only lowered and only in order to avoid extreme predetonation or knocking at full load throughout the majority of its speed range. In cases where either the combustion method or engine architecture required the use of a general cylinder object, as many properties as could be carried over, were. Fuel is directly injected into the cylinder unless the concept requires otherwise. Deviations will be discussed in their respective sections.

3.2.3 Valves

The valve flow coefficients vs. lift profiles are also left untouched between all engines. The lift profiles are unchanged in their general shape (i.e. the order of the polynomial that defines the lift curve is untouched), but are allowed to be scaled in terms of both lift and duration. Due to the varied nature of the gas exchange processes in each of these concepts, proper valve timing has a very large impact on their very theory of operation. Forcing them to operate with valve durations and lifts optimized for a conventional four-stroke engine is unreasonable. VVT is implemented in all engines on all poppet valves. These parameters are calibrated with equal resolution and vary with both speed and load throughout each engine's entire operating range. At all loads below the maximum, the valve timing which reduces the BSFC to a minimum while still allowing for fewer than 25% burned residuals in the cylinder is selected. At full load the valve timing which maximizes engine output is selected.

3.2.4 FMEP

The FMEP of each engine is dependant on its architecture. This is modelled in GT-Power using the Fischer-FMEP object which calculates the values based on the engine's cycle averaged coolant and oil temperatures, speed, and BMEP. The user inputs known FMEP values at 0 bar BMEP at a low and a high engine speed. The object then calculates what the values should be depending on the current engine operating conditions. The first obstacle was how to scale the FMEP for each engine. According to Figure 13-8 in Heywood[12], FMEP is strongly correlated to engine speed, loosely correlated to stroke to bore ratio, and not correlated to displaced volume. Since the stroke to bore ratio is the same for all of the engine concepts, this just leaves their FMEPs to be scaled based upon their architecture, that is, the quantity of each component type it has.

A friction breakdown study from a production engine provided measured FMEP values from the piston assembly, crankshaft, valvetrain, water pump and alternator (unloaded), oil pump, and fuel injection pump. The scaling is done by calculating a weighted ratio for the concept's FMEP compared to that of the measured engine. The ratio is weighted based off of the proportion of components from each category between the concept and measured engine and the contribution those components provided to the overall friction. The number of strokes between the two engine types for one cycle is also used as a scaling factor. For example, if the concept has twice as many of each engine component but half the number of strokes, the FMEP remained unchanged from the measured engine's value.

3.3 Baseline

The baseline engine is the standard to which all the concept engines are compared. It is created with the intent that it should be representative of a production engine in terms of its performance. Therefore its torque curve is designed to have a smooth transition from low to high engine speed with peak torque occurring in the middle of the speed range. It is an inline two-cylinder, four-stroke engine with four poppet valves per cylinder. The cylinders fire with 360° of separation. This layout allows for a direct comparison of expected fuel consumption in a vehicle since it shares the same displaced volume, 0.984 L, of all the engine concepts. MEPs are very useful for comparing engines to each other, but in terms of application into the same vehicle, the engine's performance at a certain torque and speed is what is important. By having the same displaced volume, both of these comparisons can be made with just a single MEP plot. This configuration also shares the same instantaneous torque profile of the firing cylinders per cycle. The only exception to this is the Recombusiton engine which has twice as many. Since the engine is forced to run at a constant speed, negating any inertial effects, this can be scaled in duration for comparison.

3.4 Over-Expansion

Due to the limitations in GT-Power, the ideal theory of operation as described in Section 2.2.4 has to be modified. The FKFS object cannot predict combustion in a prechamber. Non-predictive combustion with a quasi-steady cylinder volume with ports connetting it to other cylinder objects is also not possible. No matter the imposed combustion, GT-Power is hard coded to terminate combustion the instant any exiting valves open. Since the valves between the prechamber and cylinders would have to be open during the entire combustion duration, it is clearly not possible to simulate this engine in its intended form. The compromise, then, is to simulate it in a form as similar as possible. This means that the transfer and sharing of the combustion gases must start after the majority of the combustion process is completed. Not only does this mean the transfer valve opening needs to be retarded, but the expansion cylinder must lag by the same offset, so as to minimize the initial volume the gases expand into. With this timing convention, the expansion cylinder will be at TDC when the transfer valve opens which occurs after the majority of the fuel (MFB>90%) has been completed.

The two outer firing cylinders operate on a four-stroke cycle and have four poppet valves per cylinder. One of those is a transfer port which connects to the two-stroke expansion cylinder. The transfer port valves leading into the expansion cylinder are check valves actuated via a pressure differential between the two volumes. The average pressure drop across the similar sized poppet valves was measured on the baseline engine and to that pressure drop, the maximum flow coefficient of the poppet valve was assigned. This gives the two valve types similar maximum flow properties. Values between 0 and the maximum pressure drop are calculated internally by linear interpolation. Check valves were used leading into the expansion cylinder since GT-Power does not allow a four-stroke valve actuation schedule attached to a two-stroke cylinder. The expansion cylinder has one poppet exhaust valve which brings the total to two check valves and one poppet valve.

3.5 Recombustion Cycle

Due to the nature of the combustion processes, the FKFS cylinder object cannot be used since it supports neither HCCI nor stratified charge combustion. Therefore the burn durations and anchors are modelled with a Wiebe curve based on measured data. Thomas Johansson et al. investigated this very relationship in a joint study between Lund University, in Lund, Sweden and the late car manufacturer, SAAB Automobile Powertrain AB. They tested a four-cylinder turbocharged engine modified to run with HCCI combustion. Their cylinder geometry is similar to that used in the baseline engine, but the in-cylinder turbulence and knock tolerance is unknown. They calibrated the operating map for MBT between 1000 to 3000 *rpm* and 1 to 6 *bar* IMEP. In terms of the 10-90% MFB duration, they found that above 2000 *rpm* it was fairly constant in terms of time vs. engine speed, as follows, the duration in CAD increased with engine speed. This suggests that the degree of in-cylinder turbulence is fairly constant for that speed range.

Burn duration did increase below 2000 *rpm* which suggests that the engine was relying more on spark assist to ensure combustion at low engine speeds. They generated a curve fit for the MBT point of the 50% MFB anchor. They found that the relationship was linear with respect to IMEP and independent of speed. The final aspect they investigated was the Wiebe exponent and how that was affected throughout the operating range. It was discovered that this too was only dependent on IMEP in a linear fashion which led to another curve fit being generated.[13] The tabular burn durations and curve fit equations they generated are entered into GT-Power to model these phenomena. Since the burn duration varied non-linearly with load and that variation was also different at different engine speeds, the values throughout the load range at 3000 *rpm* were extrapolated to higher engine speeds, sticking to the convention of constant burn duration in terms of time, therefore increasing in terms of CAD. This is an assumption, but a more accurate assumption than just "smearing" the burn duration values at 3000 *rpm* to all higher engine speeds.

The stratified charge combustion process also has to be modelled based on values that have motivations behind them. The first is the heat transfer to the walls. One of the benefits of stratified charge combustion is that the combustion is insulated from the cylinder walls by the surrounding air. This reduces the temperature losses to the cooling system which would have lowered the IMEP. Otherwise, the heat transfer throughout the cycle is identical as in a homogeneous charge spark ignition engine. Unfortunately, no scientific papers could be found which investigated the topic of heat transfer modelling for stratified charge gasoline engines. Investigations into papers on heat transfer from Diesel engines were not considered since their combustion process is quite different from spark ignition engines. Therefore, a logical thought process is used to motivate the values set.

The crank angle duration during this reduced heat transfer benefit must be considered. It does not seem reasonable that a lower heat transfer coefficient should be imposed for the entire combustion process or expansion stroke. The flame growth in a homogeneous mixture is also insulated from the walls for a portion of the flame propagation. Those engines do, however, have a high degree of turbulence and mixing to spread the flame throughout the combustion chamber quickly. The convention chosen for this concept was that the heat transfer coefficient for the stratified charge cylinders would be lowered from 1 to 0.7 from the 50% MFB angle to 90° aTDC where it goes back up to 1 for the remainder of the cycle. The reason the span ends at 90° aTDC is because it is assumed that after this angle, in-cylinder turbulence will have transported the combusted gases to the cylinder walls. If this is not true, the error from this assumption is minimized by the nature of the surface area to volume ratio relationship displayed in Figure 2.4.

Searching for information about how one might model the combustion process itself only produced one paper from GM Corp. where they studied one single point in an engine's operating map. It's better than nothing, but disappointingly lacking compared to the depth of research devoted to the HCCI combustion process. Their engine also exhibited cylinder geometries similar to that used in this investigation. Their engine was a naturally aspirated four-stroke with spray-guided stratification. The intake manifold pressure was maintained at 95 kPa absolute at 2000 rpm running a lambda of 1.95. They calibrated the engine for MBT and this resulted in an end of fuel injection angle of 37° bTDC. The shortest 10-90% MFB combustion duration they achieved was 48°.[14] This is roughly twice as long as what is seen in a modern, high-turbulence engine. This makes sense, since in order to maintain the stratification the turbulence must be low, and typically with lower turbulence comes slower flame propagation. A linear extrapolation of combustion duration as with HCCI combustion is not realistic, however, since turbulence increases with engine speed and therefore the flame propagation in terms of time is not constant (in real HCCI combustion the flame initiates at several locations almost simultaneously so the dependence on turbulence is much lower). So, the ratio of burn durations at minimum and maximum engine speed compared to that at 2000 rpm is taken from the baseline engine where FKFS predicts the burn duration. The duration drops off by 23% from 2000 to 1000 rpm and increases by 33% between 2000 and 7000 rpm. Values in between these points are found through linear interpolation. Since the burn duration is approximately twice that for the baseline engine, the next question posed was if 8° aTDC was still the ideal 50% MFB angle. An optimization run at 7000 rpm (where the CAD duration is the longest) found that, somewhat surprisingly, 8° aTDC is still the ideal angle.

The architecture is a four-cylinder, four-stroke engine with four poppet valves per cylinder. This configuration is twice its basic form in order to have the same displaced volume as all the other engines. Firing intervals for the engine are every 180°. The stratified charge cylinders intake the air from the atmosphere and transfer it to the HCCI cylinders through two parallel transfer ports. The firing interval between the paired cylinders is 540° and their crank throws are phased 180° apart. After TDC in the stratified cylinder, there is one stroke for the expansion, another for the shared exhaust and intake process, and another for the compression in the HCCI cylinder (which aligns with the intake stroke of the stratified cylinder).

3.6 4-Stroke Regenerative Split-Cycle

Since the HX in this engine concept must withstand high temperatures and large pressure differences between the hot and cold sides, it is determined that a shell and tube style HX would handle this pressure ratio best. It is believed that other heat exchangers with better surface area to volume ratios, such as those with a corrugated cross-flow configuration, would have difficulties with mechanical strength and leakage between the sides due to their construction – the layers are usually tack welded together and any pressure differential acts to separate the layers from one-another. Two versions of this HX are created to investigate the effect the initial compression ratio has on the engine's characteristics. One where the compression ratio between the displaced compression cylinder volume during one intake stroke vs. the HX volume is 1:1, and another where it is 2.17:1. This was the highest initial compression ratio that could be achieved with tube diameters that still allowed for no more than a 10 kPa pressure drop over the hot side of the HX. This limit loosely dictates a maximum volumetric efficiency of 90% at the maximum flow rate. The tube's diameter is the limiting factor for HX volume since it limits the minimum shell diameter.

The tube length was set at 100 mm, the result of rounding up from the bore spacing. The tube diameter was sized using a balance between maximizing surface area with more, smaller diameter tubes, and maintaining adequate Reynolds numbers. The average mass flow rate during the exhaust stroke at WOT and maximum engine speed is the condition where the maximum pressure drop is applied. The pressure drop is calculated with Eq. 3.1, where f_D is the Darcy friction factor, L is the tube length, D the tube inner diameter, $\bar{v}$ the average velocity, and ρ the density.

$$\Delta P = f_D \frac{L}{D} \rho \frac{\bar{v}^2}{2} \tag{3.1}$$

The Darcy friction factor is best calculated with the Colebrook equation, but it is implicit and must be solved iteratively. A common approximation is by the Moody diagram, but the accuracy in the diagram can be up to ±10%, not including additional user error. Serghides' equation has the benefit of being explicit while still being very accurate – ±0.0023% of the Colebrook equation – but at the expense of extra calculation complexity compared to referencing a Moody diagram. Serghides' formula in its entirety follows in Eq. 3.2.[15] The variables ϵ, D, and Re are the surface roughness and inner diameter in meters and Reynolds number, respectively.

$$\begin{aligned} A &= -2\log\left(\tfrac{\epsilon}{3.7D} + \tfrac{12}{Re}\right) \\ B &= -2\log\left(\tfrac{\epsilon}{3.7D} + \tfrac{2.51A}{Re}\right) \\ C &= -2\log\left(\tfrac{\epsilon}{3.7D} + \tfrac{2.51B}{Re}\right) \\ f_D &= \left(A - \tfrac{(B-A)^2}{C-2B+A}\right)^{-2} \end{aligned} \tag{3.2}$$

To clarify a previous statement, the equation is explicit if you have defined the diameter and are attempting to calculate the pressure drop it provides. The most efficient way to work backwards, as in this case, is to vary the diameter until the desired pressure drop is achieved. This is done very easily with the software program Excel. The velocity in one tube is calculated from the density and mass flow rate of the gases, and number of tubes. Since turbulent flow allows for significantly higher Nusselt numbers than laminar flow does (over one order of magnitude between the two), and therefore significantly higher convective heat transfer coefficients, the target minimum Reynolds number was 10,000, the lower limit for turbulent flow in cylindrical tubes. The resulting geometry is 16 tubes with an inner diameter of 8.5 mm and 0.5 mm wall thickness arranged in a two-level circular pattern. The shell diameter is 81 mm for the 1:1 version and 58 mm with the tubes shortened to 80 mm for the 2.17:1 version. The pressure drop through the cold side of the HX is modelled based off of the relationships from Eq. 7-48 and Figure 7-27 from Çengel.[16] On this side of the HX, the pressure drop was a result of the geometries generated from the above requirements as opposed to a target value being set. This side also contains one baffle which directs the intake air to pass perpendicular to the tubes twice before it exits into the firing cylinder.

The Nusselt numbers which drive the heat transfer in the hot side of the HX are modelled off of empirically derived formulas found in Çengel. GT-Power requires a continuous function and only allows the user to set the exponent, m, of the Colburn equation (Eq. 3.3) for laminar, transient, and turbulent regions and the turbulent coefficient, C. This is unfortunate since it is the least accurate of all the internal Nusselt (Nu) correlations.

$$Nu = C \cdot Re^m Pr^{1/3} \tag{3.3}$$

$$Nu = C \cdot Re^m Pr^{1/3} \left(\frac{\mu}{\mu_s}\right)^{(0.14)} \tag{3.4}$$

To improve the correlation, the Nusselt numbers calculated by the more accurate Sieder-Tate equation (Eq. 3.4) are used to find the exponents and coefficients which should be imposed on the Colburn equation. By this manipulation, the Colburn equation used in GT-Power will now produce results with the accuracy of the Sieder-Tate equation, so long as a constant μ/μ_s ratio is assumed. In this equation, μ is the free stream density and μ_s is the density near the surface of the tube. These values are different due to the temperature gradient of the fluid. If one would so desire, they could correlate the Colburn equation based off of the predictions from the Gnielinski equation, which is even more accurate, ±10% vs. ±25%. This equation requires a friction factor correlation for non-smooth tubes, and since one is not suggested in the text, this approach is not taken. Lastly, since these equations are really only valid for the turbulent region, the exponent for the transient region is manipulated until a continuous relationship between the laminar Nusselt number (which is a constant) and the Nusselt number at the lower turbulent limit is achieved.

On the cold side of the HX, the Nusselt numbers are not so conveniently predicted since the flow over tube banks is much more complex. Therefore, the values are based off of the empirical relationships created by Zukauskas and presented in Table 7-2 in Çengel. The coefficient and exponents are again calibrated so that the Colburn equation matches the accuracy of, this time, Zukauskas, which is ±15%.

As you can see, there are fairly broad accuracies involved in each calculation to either over or underestimate the true Nusselt number. They cannot add to each other, however, since each governs one side of the HX and the heat transfer on one side must be equal to that in the other. Short of performing physical testing on an identical HX, this is the most robust method of predicting the Nusselt numbers in the HX within GT-Power.

The compression ratio in the firing cylinder using each size of HX is found by running the engine at wide open throttle and selecting the highest ratio which avoids predetonation and allows knock to be controlled by phasing ignition timing down to an engine speed of approximately 3000 rpm.

The architecture is an inline three-cylinder engine with the compression piston lying between the two firing cylinders. The compression cylinder has two intake poppet valves with two check valves, one distributing air to each heat exchanger which lay between the compression and two firing cylinders. The firing cylinders have one intake and two exhaust poppet valves. Only one intake valve was used to achieve the desired initial compression ratio. The firing cylinder's crank pins are in-phase with each other but the cylinders fire 360° apart. The crankpin of the compression cylinder is offset from them by 180°.

3.7 2-Stroke Regenerative Split-Cycle

Since the 2-Stroke Regenerative Split-Cycle concept only has one mechanical compression stage, it is critical that the transfer port in this case is small so that adequately high compression ratios can be achieved. Because of what was learned in the 4-Stroke Regenerative Split-Cycle modelling phase, the transfer port is not modelled as a shell and tube HX. To investigate the potential of this concept, a quicker, less modelling intensive approach is adopted. A heat transfer rate is imposed on the transfer port. From this perspective it provides results based on the assumption that a HX of some architecture could achieve a certain effectiveness. To understand the impact of the HX's effectiveness on the performance of the engine, several values are used. The heat transfer rate is calculated at every timestep with the equation $\dot{Q} = \epsilon\dot{Q}_{max}$ where ϵ is the effectiveness. $\dot{Q}_{max}$ is calculated through $\dot{Q}_{max} = hA_s\Delta T$ where h is the convective heat transfer coefficient, A_s is the surface area of the transfer port, and ΔT is the difference between the exhaust gases in the exhaust port and the air in the transfer port. The convective heat transfer coefficient is determined from a Nusselt number in the middle of the transient flow region since the pulsatile motion and turbulence from the gas transfer process is believed to maintain non-laminar flow until the next gas transfer process.

Since the firing cylinders operate on a two-stroke cycle with poppet valves in the head, the exhaust stroke must be completed before the transfer valve can open, otherwise the risk for short circuiting the fuel is very high due to the large pressure difference between the transfer and exhaust ports. In order to minimize trapped residuals and avoid compressing hot gases, this also means that the exhaust valve must close around TDC, leaving the transfer valve to open around the same time. The air must be transferred very quickly since the transfer valve must be closed before combustion begins both for GT-Power to function properly and to minimize the initial volume the combustion can expand into. Having a long transfer valve duration pushes the 50% MFB point to very late CADs which results in very low peak cylinder pressures and reduces the degree of expansion the combusted gases experience. A preliminary transfer valve duration is set at 20° and a maximum lift of half that of the normal profile, since it must provide this lift when the piston is near the top of its stroke. Since detailed geometries are not created for these engines it is assumed that this relationship is mechanically possible.

Due to unknown difficulties, possibly inherent to the timing conventions, the FKFS cylinder object could not be implemented in this model. Instead, a Wiebe curve is imposed based on combustion durations which are modelled based on results obtained from the baseline engine. The FKFS cylinder object in that model is used to calculate the burn duration with the 50% MFB anchor set at 30° aTDC, what is believed to be the earliest possible with the aforementioned valve duration. As expected, the burn duration is longer for delayed combustion.

This engine is composed of four cylinders each with 4 poppet valves, and with a crank pin offset between each pair of compression and expansion cylinders set at 180°. It has two intake cylinders in order to match the displaced volume of all the other engines. The firing separation in the engine is also 180°.

3.8 6-Stroke Otto-Steam

Great lengths have been taken to try and simulate the 6-Stroke Otto-Steam engine within GT-Power. Gamma technologies has been consulted extensively throughout this process to try and help with this simulation. However, it is not possible at this time to do so. The first issue is created by the requirement that this concept must be run on a six-stroke cycle but the program is hard-coded to only operate on 360° or 720° cycles. This issue is may be better defined as a difficulty, however, because there is a workaround for this. A user defined piston position vs. crank angle must be defined for six strokes within a 360° range, as would the cam lift profiles. The engine speed must then be run at one third the desired speed. Since the program, in this case, would calculate power from the force on the piston multiplied by its linear velocity, this result would be scaled properly. However, torque, any MEP, etc., would have to be recalculated by the user. Still, this issue is not absolutely prohibitive.

The biggest issues are the limitations in the cylinder model. It does not include a physical evaporation model. The way it calculates evaporation is with what appears to be an empirically derived equation very specific to gasoline fuel, and it is only valid for low injected masses. The user can impose a user defined evaporation model, but it would require the user to know how to code in the FORTRAN programming language and know how to create a physical evaporation model. This in itself could be a thesis topic.

The other option is to simulate a cylinder with a general volume object, where the instantaneous volume and the heat release rate is driven to fluctuate as it would in a cylinder, and that is something that was tried. The reason this approach was investigated is that within these volumes, the user can force it to evaporate or condense an injected liquid based on the temperature in the cylinder, but it will do so even if it is not physically possible. The liquid water to be injected was set to a temperature above the critical temperature so that it would flash evaporate upon entry into the cylinder in the beginning of the fifth stroke. However, the supercritical steam managed to chill the cylinder. That was an interesting trick! It was hypothesized that the program was taking from the air some heat of vaporization for the entire water mass even if the injected water was above the critical temperature. An investigation into this hypothesis was undertaken.

For the same injection mass flow rate of 100 g/s, and a defined initial vaporized fluid fraction of 0.5 and 0.99 (assigning either 50% or 1% of the mass a non-instantaneous vaporization), the exact same temperature drop at SOI of 648.5 K occurred over 1.1° (CAD). For a fluid fraction of 0.5 and 0.99 and an injection rate of 50 g/s, the temperature drop in both cases was 579.2 K over 1.1°. These results suggested that while the vaporized fraction does not have an influence on the results, the amount of water injected does, with less mass relating to a smaller decrease in temperature. This was the first red flag, since the initial degree of vaporization should have a direct effect on the temperature change in the cylinder. Calculating the change in energy during this period was the next step. Short hand calculations show that the change in work and heat for the cylinder are very near zero for these 1.1° and therefore can be ignored without much error. It was then just required to calculate the change in enthalpy. Just before 130°, there was 16.6 mg of air in the cylinder (as determined by instantaneous density and volume). With $c_p = 1.075\ kJ/(kg \cdot K)$, $\Delta H_{air} = -11.6\ J$ after the temperature drop. At 1500 rpm, 100 g/s of water, there were 36.6 mg of water injected in 1.1°. With a $\Delta H_w = -11.6\ J$, this predicted an evaporation enthalpy of $-316.9\ kJ/kg$. It should be noted that volume increases by ˜11% and pressure increases by ˜11% in this duration, so treating it as a constant pressure process isn't absolutely accurate. That inaccuracy doesn't matter much, however, since 773 K (the injection temperature) is beyond the critical temperature of water, which means that there was no evaporation enthalpy to be crossed for a change in pressure. Furthermore, the air is initially at an even higher temperature than 773 K, so it should have had no reason whatsoever to chill the water and dip it into the two-phase vapor region.

An inquiry was made to Gamma Technologies and they agreed that it was likely an evaporation enthalpy was being taken from the air. It turns out that the steam properties in GT-Power are not found via a lookup table, but instead with a high order polynomial curve fit. The one they provide is not valid in the supercritical region. This is why whenever water was injected, it forced the entire air mass to chill. Yet another limitation is that the user is forced to specify that only the air or only the cylinder walls are the thermal sink/source for the evaporation/condensation process. This makes sense for a 1D simulation, but an improvement would be to allow the user to blend them with a ratio.

So to summarize, GT-Power would need to be modified somewhat significantly by the user in order to be able to simulate this type of engine cycle with any amount of accuracy. As an aside, due to the extremely short time each stroke takes even at modest engine speeds, it was determined that the best way to produce power and capture the coolant and exhaust exergy was to raise the water to a temperature where it would flash boil on injection, not requiring it to absorb heat from the gases or walls which takes time. The exergy in the cooling system would have first been used to raise the water temperature to near 373 K. The exergy in the combustion exhaust gases would then be used to raise it beyond the critical temperature, 647.14 K, and higher, depending on the available amount of exhaust exergy and temperature difference.

Table 3.1: Selected standard characteristics maintained between all engines unless otherwise stated.

GEOMETRY	
Cylinder	
Bore	82 mm
Stroke	93.2 mm
Compression Ratio	12.5:1
Max mean piston speed	21.7 m/s
Intake	
Max throttle diameter	Smallest whole mm where $BMEP = maxBMEP - \leq convergence\ tolerance$
Max pressure drop over filter element	0.2 kPa
Volume	1.5*Displaced Volume +/- 10%
Runner flow area	Combined port flow area
Valve diameter	26.5 mm
Port length	85 mm
Port wall temperature	450 K
Port heat transfer multiplier	1.5
Inlet pressure	1 bar absolute
Exhaust	
Primary runner flow area	Combined port flow area
Valve diameter	22.5 mm
Port length	80 mm
Port wall temperature	550 K
Port heat transfer multiplier	1.5
Back pressure	1 bar absolute
CONVERGENCE	
BMEP	Variance $\leq$0.05 bar for 3 consecutive cycles
OPERATION	
Max Residuals at cycle start	25%
Max exhaust port temperature	1223 K
50% MFB	8° aTDC
Lambda	1 (<1 for EGT control)

4

Results and Discussion

Since there are a number of engine concepts, the discussion for each will directly follow the presentation of the results so that the outcome of the investigation is still fresh in the reader's memory. All line plots have an x-axis resolution of 500 *rpm* with an exact placement of y-values. All non-comparative contour plots have a resolution of 0.5 *bar* BMEP and 500 *rpm*. The exception are the uppermost values of BMEP which may lie at intermediate values as determined by the maximum capabilities of the engine at that speed. All comparative contour plots will have a constant resolution equal to that stated above, and at exact BMEP locations equal to that determined by the baseline engine. This is because when the concept's performance is compared to the baseline's, if the BMEP value of the concept engine varies more than 0.25 *bar* (half the resolution) from that of the baseline, the two engines are deemed to not be running at the same load point and no data is shown for that point in the map. Where this occurs only the white background will appear.

4.1 Baseline

4.1.1 Results

Figure 4.1 shows the baseline engine's BSFC throughout its entire load map. It has a minimum value of 201.5 $g/(kW \cdot h)$ at 13 *bar* BMEP, 3000 *rpm*. The peak BMEP of the engine is 13.14 *bar* at 3500 *rpm*. The rise and plateau of values at and below 4 *bar* and above 4000 *rpm* is due to the fuel enrichment necessary to maintain adequate EGTs. A slight leveling off of values above this engine load can be seen for the same reason. This trend shows that the BSFC is more strongly tied to the enriched fuel-air mixture than the increasing FMEP that comes from increasing engine speed. Figure A.1 and A.2 in the appendix show the conformance of the engine to the maximum EGT and residual BMF values, respectively. The EGT is too high at one load point; 1 *bar* at 6000 *rpm*. This load point is very uncommon in operation and is easily fixed by further enriching the fuel-air mixture. Recreating the entire load map is very simulation intensive, however, and the return on time invested by fixing a single uncommon load point is negligible. The lowest engine speed where fuel enrichment begins is 4000 *rpm*. Below this speed, all imposed lambda values are 1.

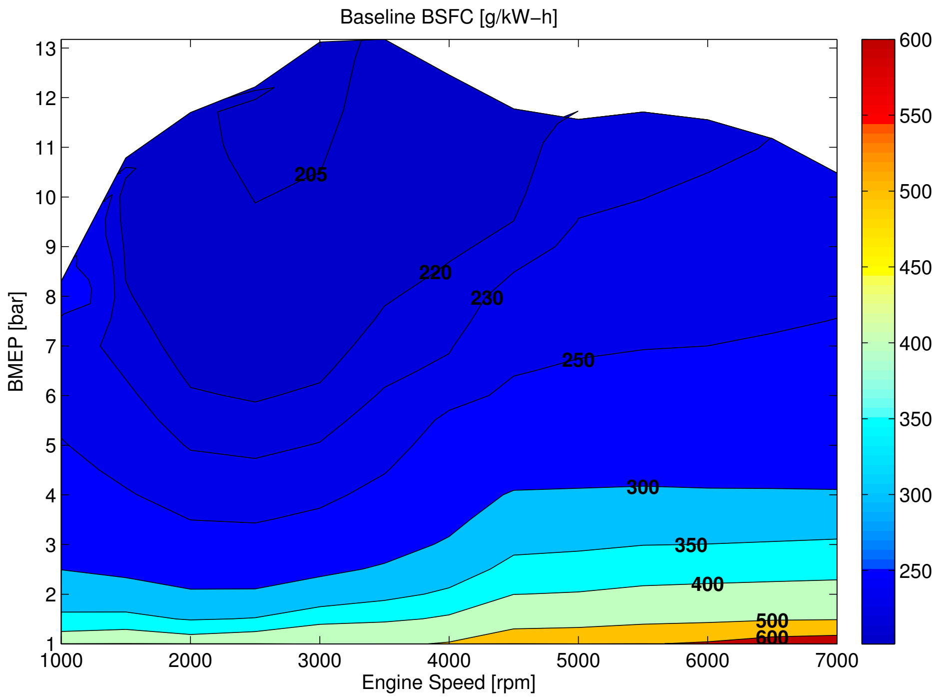

Figure 4.1: BSFC for the baseline engine throughout its entire load map.

The maximum brake power and torque, and VE throughout the engine speed range are displayed in Figure 4.2. The peak power, torque, and VE values are 80.7 hp, 103.2 $N \cdot m$, and 93.2%, respectively. This gives the engine specific outputs of 82.0 hp/L and 104.9 $N \cdot m/L$.

4.1.2 Discussion

The minimum BSFC for this engine is fairly low; it translates to a brake fuel conversion efficiency ($\eta_{f,b}$) of 40.2%, which to the author's knowledge is unprecedented for a homogeneous charge spark ignition gasoline engine sized for automotive applications. The volume-specific performance figures and VE are all reasonble values, however. This suggests that perhaps the FMEP for the engine is under-predicted. This could be from the manner in which FMEP was scaled from experimental data. Another source of error could come from the way the Fischer-FMEP object predicts the impact that BMEP has on FMEP. With smaller connecting rod length to crank radius ratios, the connecting rod axis will intersect the cylinder axis at larger angles throughout the stroke, placing more

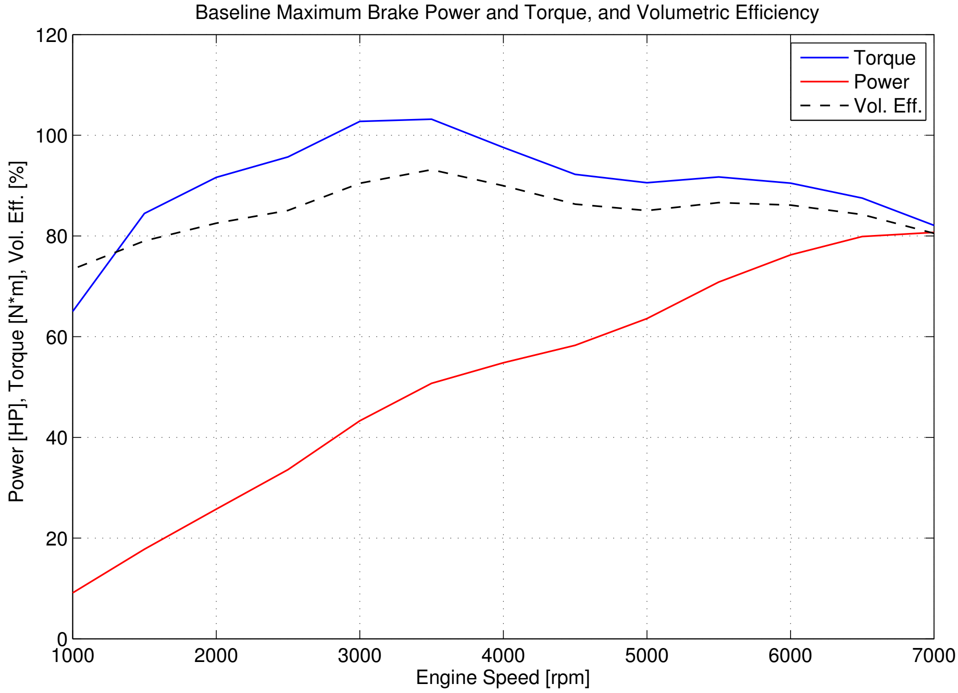

Figure 4.2: Maximum brake power and torque, and volumetric efficiency for the baseline engine.

side loading into the cylinder walls, creating more friction. The Fischer-FMEP object does not allow the user to provide this ratio and it is not clear if the FMEP increases with increasing BMEP as much as it should. This is why the accuracy of this friction model is brought into question.

In the end, this high efficiency does not raise much cause for concern, however. The reason for setting all of the metrics which each engine must conform to and all of the common attributes shared between them is to create a comparative analysis. Any deviation from what is realizable in the baseline engine will likewise be represented in the other engine concepts as well. The BSFC map is presented here not as a suggestion of what real world values should be expected from a prototype of this engine, but rather to show the distribution of values throughout the load map.

4.2 Over-Expansion

4.2.1 Results

The BSFC values throughout the full load map of the Over-Expansion engine are displayed in Figure 4.3. The minimum value is 209.3 $g/(kW \cdot h)$ ($\eta_{f,b} = 38.6\%$) at 12.5 *bar* BMEP, 2500 *rpm*. The peak BMEP for this engine is 13.15 *bar* at the same engine speed. Figure A.3, A.4 and A.5 in the appendix show the conformance of the engine to the maximum EGT and residual BMF values, respectively. The temperature in the exhaust ports are well below the upper limit of 1223 K, and this is achieved without any fuel enrichment. The temperature in the transfer ports, however, is very high throughout most of the load map. This is expected, however, since the cylinder timing dictates that the transfer valves and ports will be exposed to post-combustion temperatures.

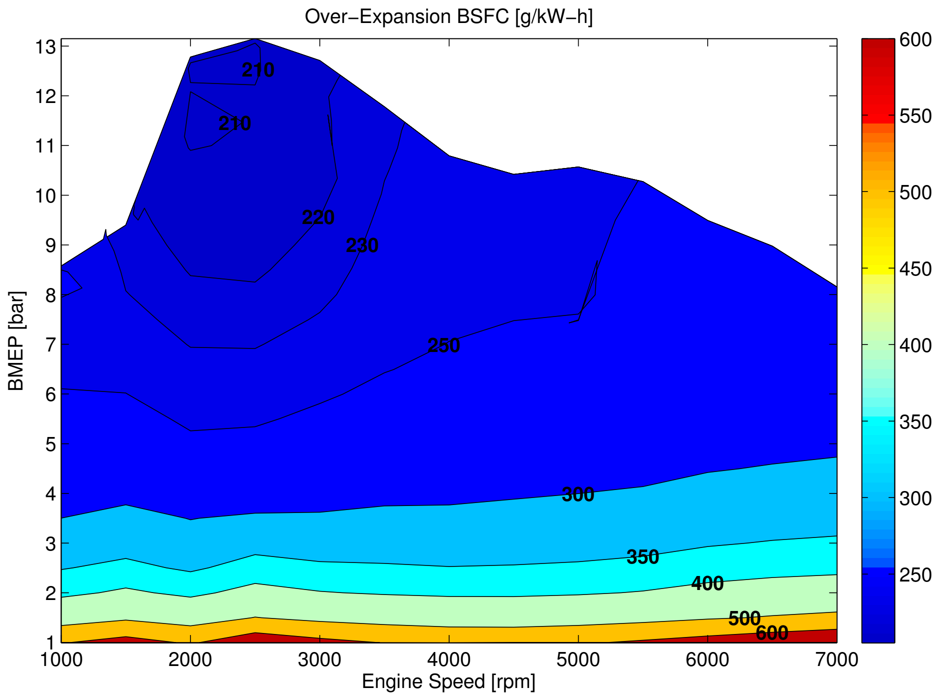

Figure 4.3: BSFC for the Over-Expansion engine throughout its entire load map.

In Figure 4.4, the percent different in BSFC between the baseline and Over-Expansion engines is shown. Positive values represent an increase in fuel consumption over the baseline engine while negative values represent a decrease. The first point of order is to address the shape of the plot. As mentioned in the beginning of this chapter, operating points which deviate too far from those of the baseline are ignored. There is significant deviation in some parts of the map and the reason for this is the throttle controller. It is unknown why it got stuck at some values in the upper portion of that map.

Taking the engine speed of 4500 rpm as an example, after the 7.5 bar BMEP load, it kept creating data for 7.79 bar when it was supposed to be targeting 8.5, 9, and so on. That value stuck until it hit the 11 bar load point, at which the engine can only reach 10.14 bar. The reason the non-comparative maps do not have holes is the two distant points are being interpolated inbetween which fills in those maps. These holes in the data are unfortunate, but a least they do not occur at low loads and engine speeds where one would typically expect the engine to operate most frequently. In this region the Over-Expansion engine consumes between 40% and 10% more fuel than the baseline engine. At higher loads, the difference is reduced to 5%. Below 4 *bar* BMEP, the gases in the expansion cylinder are expanded to sub-atmospheric pressures between 0.75 and 1 *bar* absolute. This negative work contributes to the increase in fuel consumption seen in this part of the load map.

Above 4000 *rpm* between 2 and 4 *bar* BMEP the Over-Expansion engine shows either no difference, or a slight reduction in fuel consumption when compared to the baseline. This is one area in the baseline engine's fuel enrichment table with the lowest lambda values. Examining the baseline's EGTs suggests that a finer resolution in the fuel enrichment table could mean that the Over-Expansion engine would have higher BSFC values throughout its entire load map since there is quite a safe margin left to the maximum temperature. Regardless, the improvement in efficiency is in an inefficient and uncommon region of the load map.

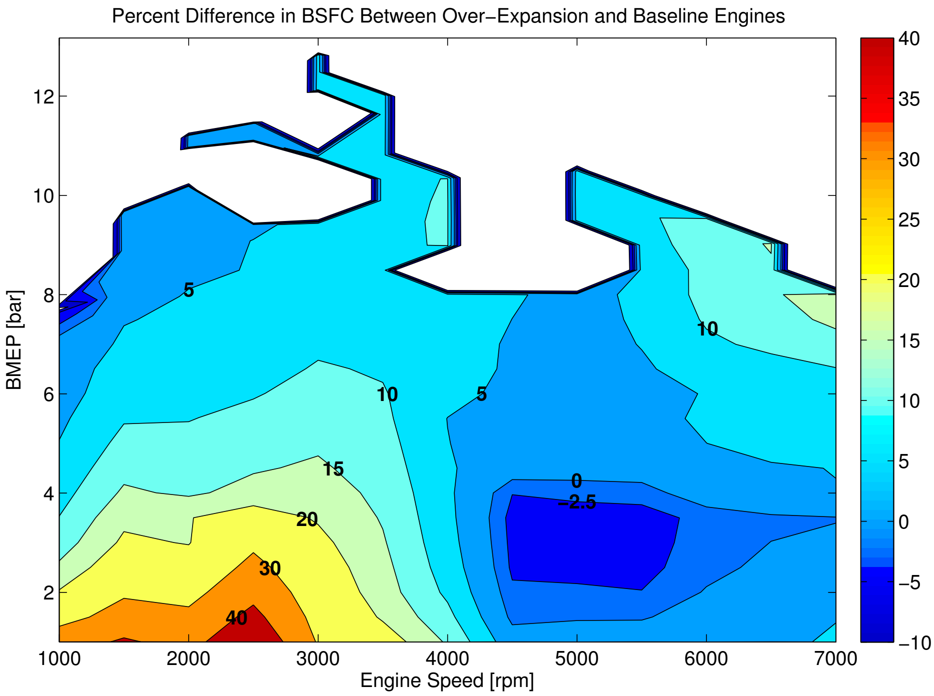

Figure 4.4: Percent difference in BSFC between the baseline and Over-Expansion engines. Positive values represent an increase in fuel consumption over the baseline engine, negative values a decrease.

The maximum brake power and torque, and VE throughout the engine speed range are plotted in Figure 4.5. The VE is measured for the firing cylinders since they take in the air from the atmosphere. The peak power, torque, and VE values are 64.1 hp, 103.0 $N \cdot m$, and 93.6%, respectively. This gives the engine specific outputs of 65.1 hp/L and 104.7 $N \cdot m/L$.

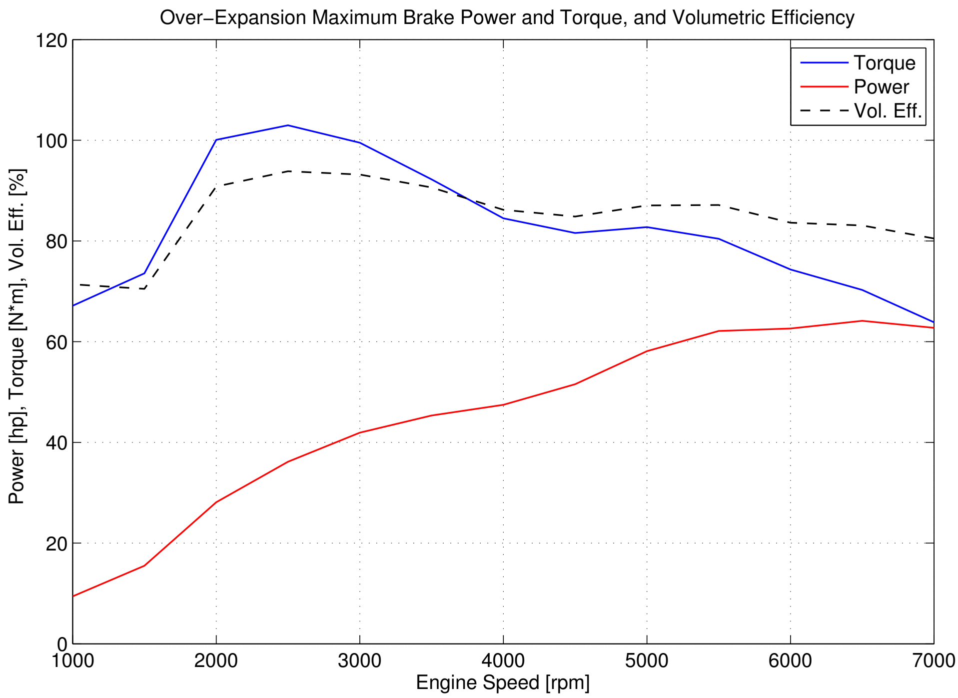

Figure 4.5: Maximum brake power and torque, and VE for the Over-Expansion engine. The VE is measured for the firing cylinders since they take in the air from the atmosphere.

4.2.2 Discussion

One of the first obvious drawbacks about this type of engine configuration and timing is the extreme temperature the transfer valves are exposed to. Some of the old compound engines previously studied had water cooled transfer valves and it appears that either that method or some exotic materials would be required. This would bring with it similar heat losses those engines experienced. The heat losses to the transfer port are also high since the temperature difference is near 1000 K between the walls and the gases, depending on the load point. This temperature loss manifests itself in a lower pressure in the expansion cylinder, obtaining less positive work. One other loss comes from transferring the very hot post-combustion gases at choked flow through the transfer port due to the high initial pressure difference. Since the blow down cannot happen instantly, by the time pressures have equalized between the two cylinders, the expansion cylinder is at a larger volume than when the transfer valve opened. Instead of that blowdown pressure acting on both pistons, it was trying to force its way through the transfer valve. The final significant detriment to this engine is its FMEP, which is approximately 1.5 times that of the baseline. This comes from the additional piston and valves.

It is evident that the expansion cylinder is at best only just able to barely cancel out the added friction and flow losses the architecture brings with it when considering a small portion of the load map. These findings fall in line with the historical compound engines described earlier. When considering low speed, low load operation, the engine is significantly less efficient than the baseline.

4.3 Recombustion

4.3.1 Results

The BSFC values throughout the full load map of the Recombustion engine are displayed in Figure 4.6. The minimum value is 227.9 $g/(kW \cdot h)$ ($\eta_{f,b} = 35.6\%$) at 10.0 bar BMEP, 3000 rpm. This is also the peak BMEP for the engine. Figure A.6, A.7 and A.8 in the appendix show the conformance of the engine to the maximum EGT and residual BMF values, respectively. The temperatures in both the transfer and exhaust ports are well below the upper limit, and this is achieved without any fuel enrichment.

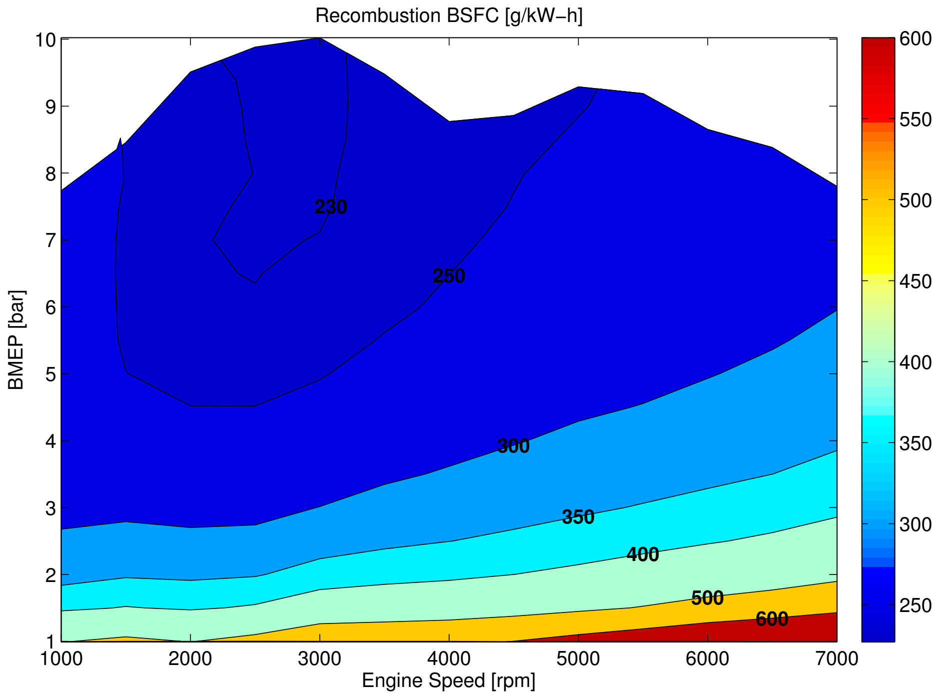

Figure 4.6: BSFC for the Recombustion engine throughout its entire load map.

In Figure 4.7, the percent difference in BSFC between the baseline and Recombustion engines is shown. Positive values represent an increase in fuel consumption over the baseline engine while negative values represent a decrease. The Recombustion engine consumes between 5% and 15% more fuel throughout most of its load map, with a few exceptions. At and around 3.5 bar BMEP, 4500 rpm, the Recombustion engine has an identical or slightly reduced fuel consumption. This is partly due to the resolution of the fuel enrichment table for the baseline engine. Examining the baseline's EGTs suggests that a finer resolution in the fuel enrichment table could mean that the Recombustion engine would have higher BSFC values throughout its entire load map since there is quite a safe margin left to the maximum temperature.

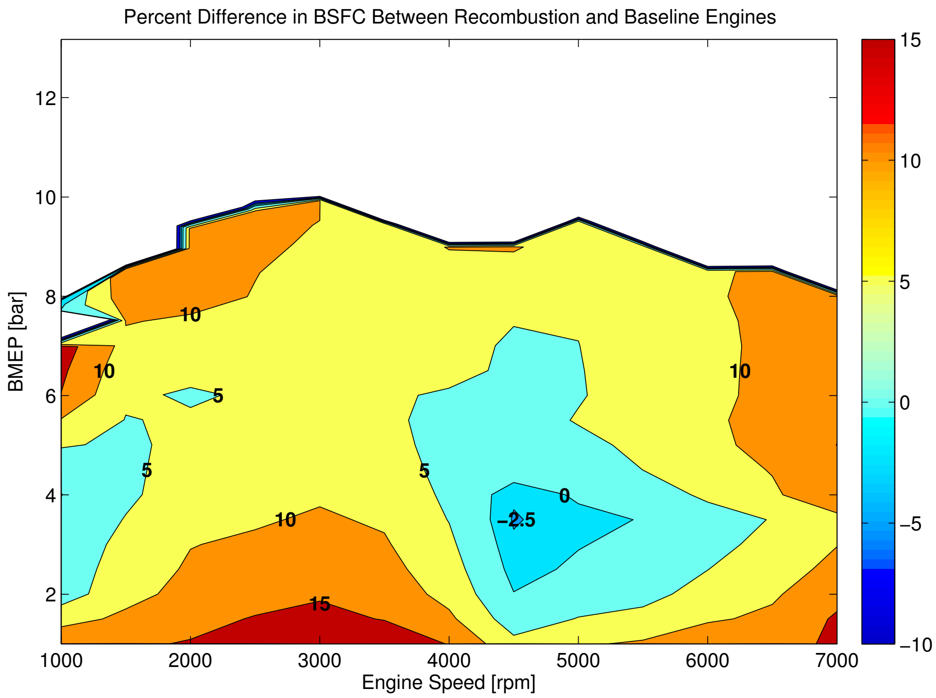

Figure 4.7: Percent difference in BSFC between the baseline and Recombusiton engines. Positive values represent an increase in fuel consumption over the baseline engine, negative values a decrease.

The maximum brake power and torque, and VE throughout the engine speed range are plotted in Figure 4.8. The VE is measured for the stratified charge cylinders since they take in the air from the atmosphere. The peak power, torque, and VE values are 60.0 hp, 78.5 $N \cdot m$, and 79.6%, respectively. This gives the engine specific outputs of 61.0 hp/L and 79.8 $N \cdot m/L$.

4.3.2 Discussion

One of the drawbacks of this engine concept are the losses in the gas exchange processes. This is due in-part to the architecture of the engine as well as the cycle itself. Examining the cycle first, the flow losses are higher than in the baseline engine because of the number of valve stages the gases must pass through before exiting the engine. There are four stages of valves (intake, transfer out, transfer in, exhaust) as opposed to two (intake, exhaust) and since the flow coefficients are well below 1, each successive stage adds

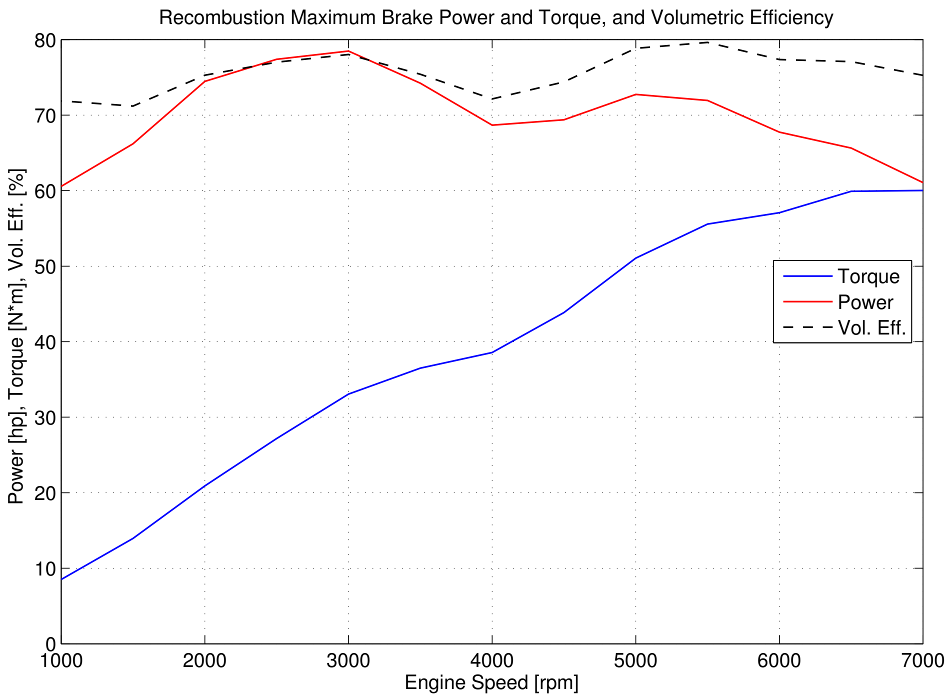

Figure 4.8: Maximum brake power and torque, and VE for the Recombustion engine. The VE is measured for the stratified charge cylinders since they take in the air from the atmosphere.

approximately the same resistance and effectively doubles the flow losses between the intake and exhaust manifolds. It should be noted that a doubling of flow losses within the engine does not mean that the volumetric efficiency should be halved. The added losses take place in the transfer ports between the cylinders where the restriction creates a negative work. With proper VVT, the detrimental effects from this restriction like back flow in the intake port due to pressure differences can be mostly avoided, but still, an unaffected VE should not be expected.

Apart from the cycle, part of the flow losses and decrease in VE are inherent to the piston motions within the cylinder. Since connected cylinders have crank pins phased 180° apart (but with a firing phasing of 540°), the way in which the instantaneous velocities fluctuate with respect to eachother add to the flow losses. As you will recall from Section 2.2.1, pistons travel slower in the lower 180° of the stroke than in the upper. What happens as a result of this is a reduction in the shared volume between the two cylinders, which means that the exhausting piston has to slightly compress the gases into the HCCI firing cylinder. In the first half of the exhaust stroke, the opposite occurs and the gases can actually expand into the HCCI cylinder. But, unfortunately, since the intake valve has to open after the point where the piston has to compress the gases into the HCCI cylinder, a detrimental pressure difference across the intake valve is bound to occur. This reduces the VE. The relationship of this shared volume is shown in Figure 4.9. As an example, if 4π is TDC of the exhaust stroke for the exhausting cylinder, the shared volume is at its minimum. A quarter of a revolution before that, the shared volume is at its maximum. This makes sense since the pistons are farther than half way down the cylinder when they are 90° (or $\pi/2$ radians) from TDC or BDC and after this point the exhausting piston starts travelling faster upwards than the intaking piston is travelling downwards. This causes the reduction in shared volume between 3.5π and 4π (or 540° and 720°).

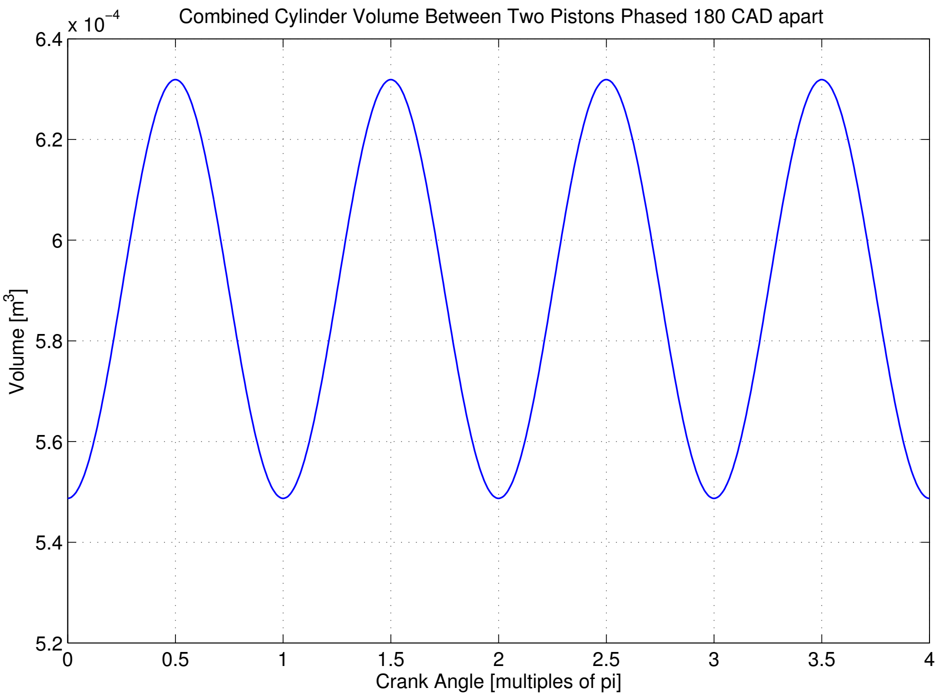

Figure 4.9: Shared cylinder volume between two connected cylinders which have crank pins phased 180° apart. Connecting port volume is not included since it is constant. 0, 2, and 4π are TDC for the exhausting cylinder.

The other detriment to this engine's performance is its increased friction. It has twice as many of some major components and therefore nearly twice the FMEP as the baseline engine. It is slightly less than double because components like main bearings are not exactly doubled between a two and four cylinder engine.

One characteristic of this engine may over shadow all of the drawbacks above. It seems unlikely that this engine could fire properly. Remember that in this engine, the burn rates are imposed, in other words, combustion is guaranteed in the simulation. The issue is it appears that the in-cylinder temperature at IVC for the HCCI cylinder is too high to allow for properly phased combustion. Roy Ogink found through experimental testing that in an engine with a compression ratio of 11:1, a temperature of 520 K at IVC was the upper limit for early combustion timing.[17] Taking 3000 *rpm* as an example in the Recombustion engine, in cylinder temperature at IVC is 765 K at 1 *bar* and 860 K at 10 *bar* BMEP. Even at 1000 *rpm*, where heat losses to the walls are the greatest, the temperature only gets down to 659 K. Typically, this temperature is controlled with valve overlap in a normal HCCI engine, regulating the amount of internal EGR. However, since part of the point of this succession of combustion process is to have stoichiometric exhaust products, no exhaust gases can be vented before the HCCI cylinder because they are very lean. It may be possible to force fresh air into the transfer port after the stratified charge cylinder has been closed off, but that would require a boosting system, which is not part of this study. There may also be other ways to cool the gases before the HCCI IVC, but one must be careful not to increase the cooling losses in doing so. Since increased compression work is also a result of this engine compressing the hot gases from one cylinder, the reduction in this negative work may more than offset any cooling losses incurred. It is one possible topic for further investigation.

4.4 4-Stroke Regenerative Split-Cycle

4.4.1 Results

The BSFC values throughout the full load map of the 1:1 initial compression ratio version of the 4-Stroke Regenerative Split-Cycle (4SRSC) engine are displayed in Figure 4.10. The minimum value is 280.4 $g/(kW \cdot h)$ ($\eta_{f,b} = 28.9\%$) at 7.5 *bar* BMEP, 2000 *rpm*. The peak BMEP for this engine is 7.94 *bar* at 3000 *rpm*. Figure A.10 in the appendix shows the conformance of the engine to the maximum residual BMF value allowed. Figure A.9 shows that the EGTs, however, are significantly above the allowable limit. Fuel consumption is extremely high over 4000 *rpm* due to very rich mixtures being imposed, and still the EGTs are excessively high – well over 1250 K at the majority of load points. The 4SRSC engine may need exotic materials to withstand the heat. At 7000 *rpm*, temperatures of 1300 K still occur at lambda values of 0.82 (AFR = 12:1). By this measure, the engine is not compliant to the standards imposed on all the engines. Further mixture enrichment is not conducted since the trend in BSFC is already quite obvious.

In Figure 4.11, the percent different in BSFC between the baseline engine and the version of the 4SRSC engine with an initial compression ratio of 1:1 is shown. Positive values represent an increase in fuel consumption over the baseline engine. This engine consumes between 20% and 80% more fuel than the baseline engine. The fuel mixture enrichment only impacts the consumption above 3000 *rpm*. At and below that speed, a lambda value of 1 is imposed.

The maximum brake power and torque, and VE throughout the engine speed range are plotted in Figure 4.12. The VE is measured for the compression cylinder since it takes in the air from the atmosphere. The peak power, torque, and VE values are 43.4 *hp*, 62.2 $N \cdot m$, and 87.1%, respectively. This gives the engine specific outputs of 44.1

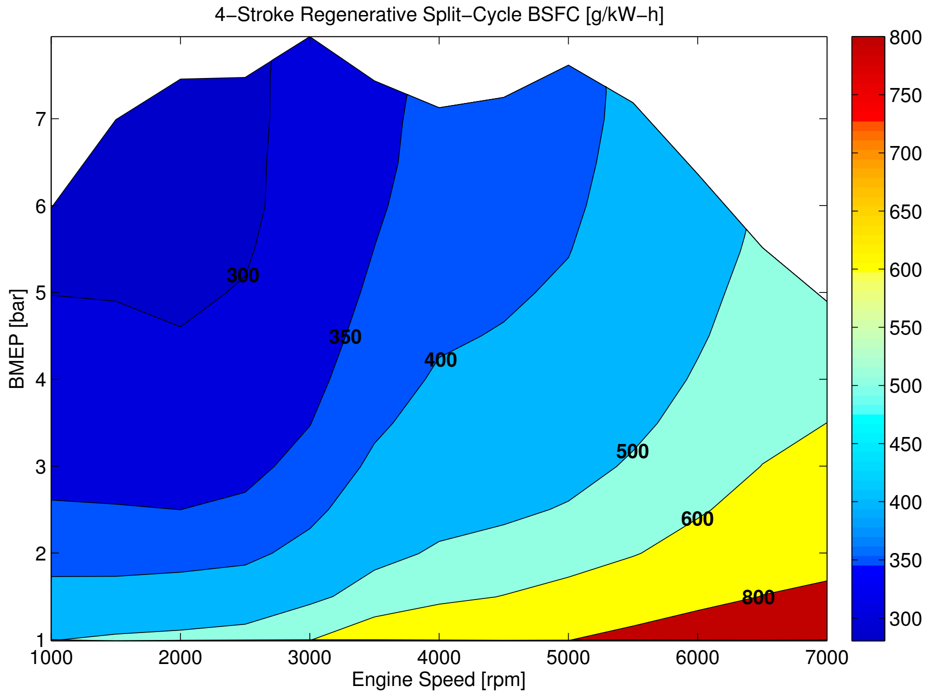

Figure 4.10: BSFC for the 1:1 initial compression ratio version of the 4SRSC engine throughout its entire load map.

hp/L and 63.2 $N \cdot m/L$.

In Figure 4.13, the percent different in BSFC between the baseline engine and the version of the 4SRSC engine with an initial compression ratio of 2.17:1 is shown. Positive values represent an increase in fuel consumption over the baseline engine. The maximum BMEP was slightly higher for this version at 8.5 bar. This engine consumes between 17% and 80% more fuel than the baseline engine. The fuel mixture enrichment only impacts the consumption above 3000 rpm. At and below that speed, a lambda value of 1 is imposed.

4.4.2 Discussion

Regarding the BSFC figures, to put the fuel consumption maps into perspective, lambda values of 1 were imposed at 3000 rpm despite EGTs being too high. This engine speed is likely in the driving cycle of the vehicle and therefore it must run at lambda 1 in order for the catalysts to operate efficiently. The results presented above must come with the realization that exotic materials will likely be necessary in the exhaust valves and other components in the exhaust stream.

There are several losses in the 4SRSC engine. Some of these losses are due to the processes during the cycle, and others are due to the architecture of the engine which

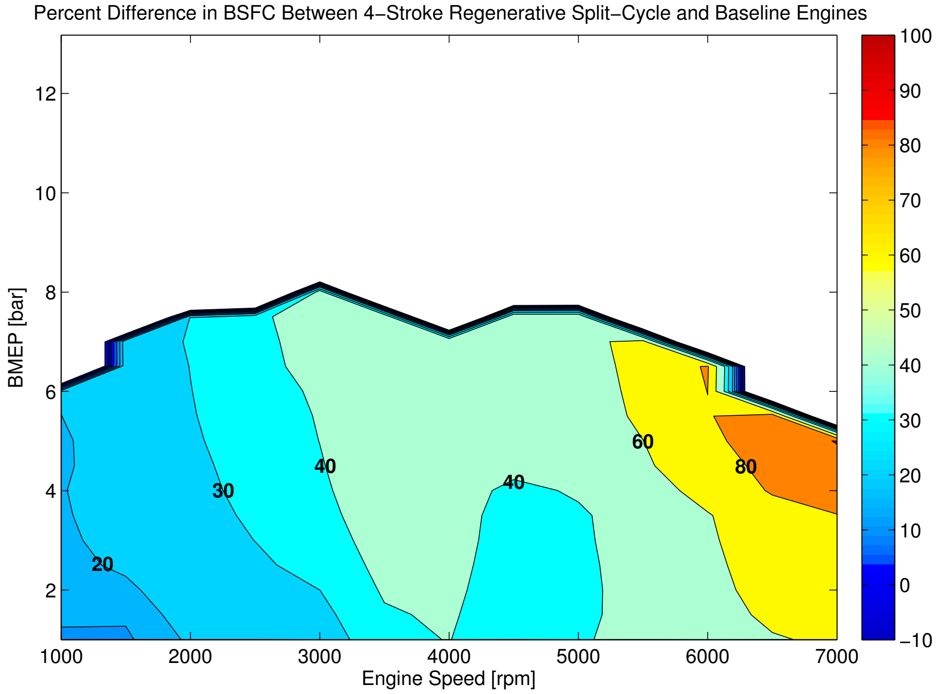

Figure 4.11: Percent difference in BSFC between the baseline and 1:1 4SRSC engines. Positive values represent an increase in fuel consumption over the baseline engine, negative values a decrease.

increases flow losses and friction.

Focusing first on the processes: The air which is pressurized and heated in the HX is expanded during the firing cylinder's intake stroke, exposing the air to the full surface area of the cylinder, where the coolant jackets in the head and cylinder walls along with the piston will absorb some of its heat. This effectively transfers some exhaust exergy to the coolant system where it is then lost to the atmosphere. The air is then recompressed, and since the air is still quite hot, it takes extra work to compress this hot air mass when compared to the compression process of a normal Otto cycle engine since the specific heat ratio of the air is higher. Another drawback is the very short ignition delay of the fuel caused by the high average intake and compression temperatures. End of fuel injection had to be phased to 90° before top dead center to avoid extreme knocking. It is not clear if it is still possible to create a truly homogeneous mixture with the injection ending this late. Setting 90° as the limit to the end of injection, the only other way to avoid knock is to reduce the compression ratio in the firing cylinder. This causes a somewhat self-exacerbation of knocking. As the compression ratio is reduced, the exhaust gas temperatures rise since they are not expanded as fully as with high compression ratios. These even hotter exhaust gases increase the intake temperatures further via the HX. This requires a further reduction in compression ratio which again

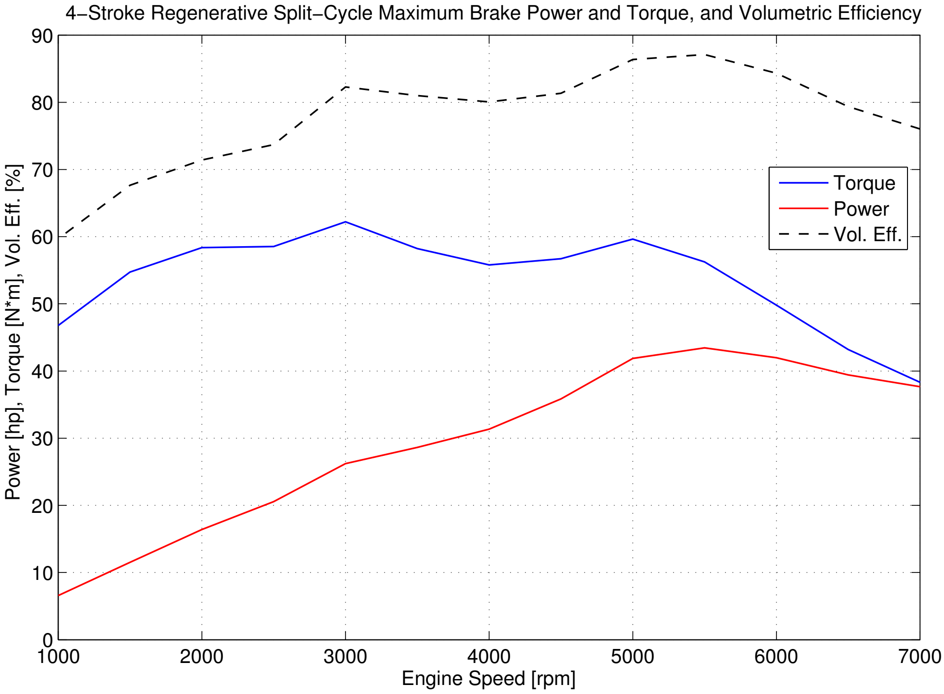

Figure 4.12: Maximum brake power and torque, and VE for the 1:1 4SRSC engine. The VE is measured for the compression cylinder since it takes in the air from the atmosphere.

raises the exhaust temperatures. This vicious cycle can be defeated, however it requires a significant decrease in compression ratio; 33% lower than in a typical Otto engine. The resulting decrease in expansion ratio is a major cause of this engine's lower efficiency.

Onto the losses caused by the architecture: Another drawback is the reduced volumetric efficiency of the engine. As opposed to one stage of valves before the firing cylinder, there are three stages. One into the compression cylinder, one between it and the HX, and another between it and the firing cylinder. Since the intake valves have a maximum flow coefficient well below one, the flow losses stack up and reduce the volumetric efficiency and add to the pumping losses within the engine itself. Pressure drops within both sides of the heat exchanger also add to the flow losses. There is a conflicting trend in that the flow elements within the HX should have large flow areas to minimize flow losses, yet have a small volume so that pressure can build up in the heat exchanger. This causes further conflicts within the HX. As volume is decreased, so is the surface area which is supposed to transfer the heat. A smaller volume (i.e. higher compression ratio from the compression cylinder) increases the temperature of the air which decreases the temperature difference between the hot and cold side of the HX, further reducing its effectiveness. The final detrimental aspect of the HX system is that the flows are not in-phase. HXs rely on simultaneous flow through both sides to be effective. In this engine, it is possible that the exhaust gases flow through while

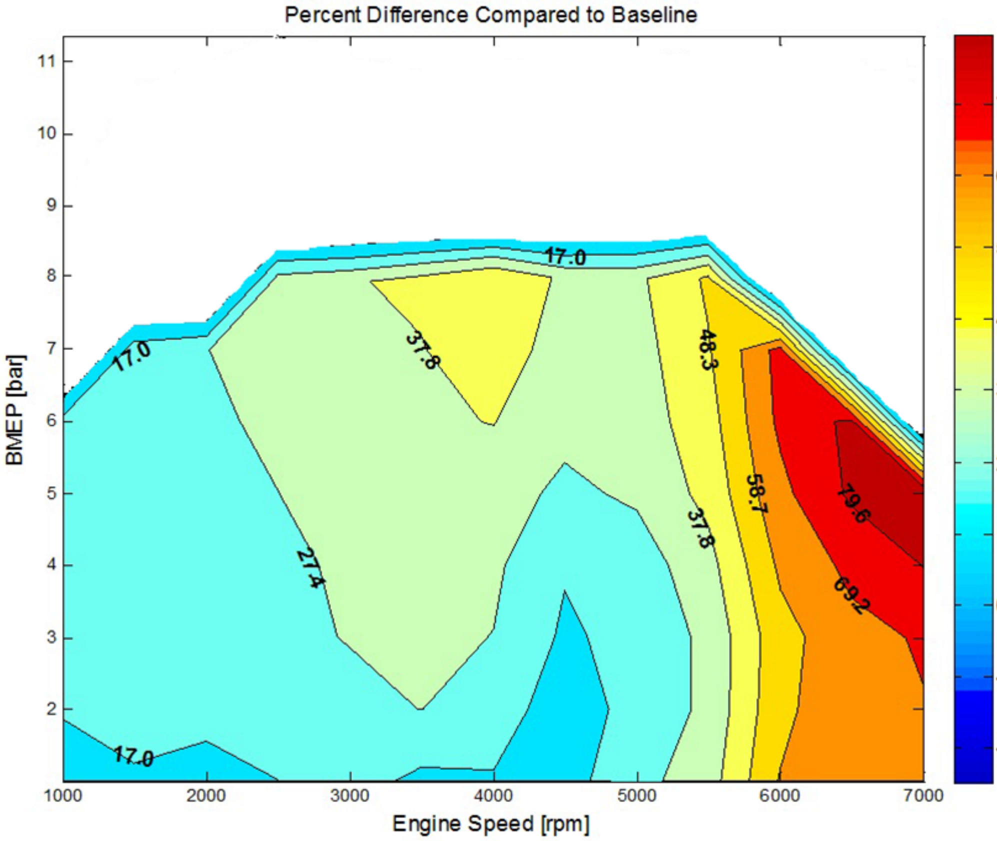

Figure 4.13: Percent difference in BSFC between the baseline and 4SRSC 2.17:1 version of the engine. Positive values represent an increase in fuel consumption over the baseline engine, negative values a decrease.

the intake air is stagnant, and the intake air enters while there is no exhaust flow. This means that there are significant durations where the heat transfer can only take place through quasi free-convection, at most with very low Reynolds numbers. The average HX effectiveness values were in the upper 20% range and lower 20% range for the 1:1 and 2.17:1 versions, respectively. The reason for the slightly improved $\eta_{f,b}$ of the version with a higher initial compression ratio is not because it reuses more exhaust energy, it does just the opposite. The low HX effectiveness is not able to transfer as much heat into the intake air. This allows the firing cylinder to have a higher compression, and therefore, expansion ratio. In short, it is more efficient because it is slightly closer in terms of operating temperatures to a standard Otto engine.

The final significant detriment to this engine's efficiency is its increased friction. It has approximately 1.5 times the FMEP of the baseline engine. This comes from the additional piston and valves.

4.5 2-Stroke Regenerative Split-Cycle

4.5.1 Results

Figure 4.14 shows the maximum BMEP for the engine in its best configuration, with the regeneration deactivated. Since the performance is so poor this is the only plot which will be shown. Many attempts and investigations have been made into how to make this engine concept perform in an acceptable manner. It appears that the very nature of this engine concept does not allow it to function well. It generates a maximum BMEP of 1.7 bar where it also has its minimum BSFC value of 1265.0 $g/(kW \cdot h)$ ($\eta_{f,b} = 6.4\%$) and maximum VE of 36%.

With the regeneration active, and at 1000 rpm where there is the most time for heat transfer to occur, the temperature in the transfer ports only increases by 10 K (<1.0%) over its 180° dwell time. This is with assuming a HX effectiveness of 25% (values typically seen for the 4SRSC engine) and multiplying the surface area of the transfer ports by a factor of ten from their basic cylindrical value. This provides heat transfer rates which average about 230 W. This meager temperature increase was cancelled out, however, once the cooler fuel was injected just before the gas transfer process.

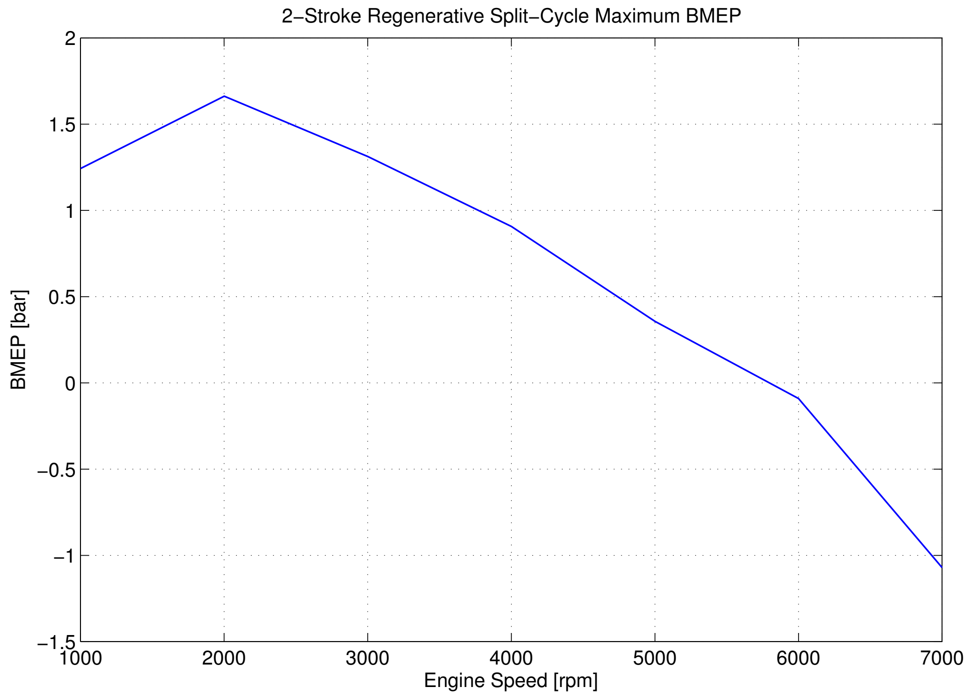

Figure 4.14: Maximum BMEP for the 2-Stroke Regenerative Split-Cycle Engine.

4.5.2 Discussion

The biggest enemies of this engine are time, limited surface area, and timing. The issues of little time and surface area mean that the required mechanical compression work remains unaffected. There is no net temperature or pressure increase by the time the transfer valve opens. Interestingly, the engine operates slightly better when regeneration is inactivated and the temperatures in the transfer port cooled slightly. Had even decent performance resulted, this phenomenon would have been investigated further.

The timing issues lie primarily in the induction process to the firing cylinder. The gases are supposed to transfer into the cylinder after the piston has already started to move down for its expansion stroke. Since combustion can only begin after the intake valve has closed, this pushes the 50% MFB point very late into the cylinder; 45°. This is exacerbated by the fact that the burn duration increases for delayed 50% MFB points. It was discovered that the peak cylinder pressure came from the release of the air from the transfer port, and not the combustion pressure that followed. Where the BMEP falls below zero, the combustion duration is so long that the valve cannot close in time and combustion does not take place. Combustion phasing could have been varied with engine speed, but the poor results at low engine speed did not warrant the additional calibration this would require.

This engine exhibited no change in friction compared to the baseline engine. This is because while it had twice as many components, it operates completely on a two-stroke cycle.

4.6 Summary

After comparing all of the studied concept engines to the baseline, it was determined that in the low engine speed range where peak efficiency is found, between 1500 and 3000 *rpm*, all of the concepts had a higher BSFC than the baseline engine. The Over-Expansion and Recombustion engines matched and bettered the BSFC of the baseline engine in some areas of the load map, but they were at higher engine speeds and fairly low loads – inefficient areas of the load map to begin with. It is also possible that with a finer resolution of the baseline's fuel enrichment table, those two concepts would have a higher fuel consumption in all points of the load map as well. The results of the key metrics of all the engines analyzed are summarized in Table 4.1. An addition to this table which was not presented before is a comparison between the engines at a common load point. An engine load of 4 *bar* (31.3 $N \cdot m$ for these engines) at 2000 *rpm* was selected as an example. By this comparison the Recombustion engine is now slightly more efficient than the Over-Expansion engine which had previously been the best of the selected concepts. Still, the baseline is the most efficient engine.

4.6.1 Closing Remarks

In order to separate the processes of these engine concepts spatially, additional hardware was needed. In some cases these components contributed to the FMEP, in others flow

Table 4.1: A summary of the performance of the baseline plus all evaluated concepts.

	Baseline	Over-Expansion	Recombusiton	4SRSC	2SRSC
Minimum BSFC $[g/(kW \cdot h)]$	201.5	209.3	227.9	279.6	1265.0
$\eta_{f,b}$ [%]	40.2	38.6	35.6	30.0	6.4
$\eta_{f,b}$ [%] @ 4 bar BMEP, $2krpm$	33.1	29.0	30.6	25.8	N/A
Peak BMEP $[bar]$	13.14	13.15	10.0	8.5	1.7
Peak VE [%]	93.2	93.6	79.6	82.8	36.0
Specific Power $[hp/L]$	82.0	64.1	61.0	45.5	4.7
Specific Torque $[N \cdot m/L]$	104.9	104.7	78.9	63.8	13.2

and heat losses. The worst of these were transfer ports and valves which added to them all. A separation in time was also necessary. In the 4SRSC engine, extra strokes and time lead to a transfer of exhaust exergy to cooling system exergy and an increased knock propensity. In the 2SRSC engine, a lack of time meant that the HX could not raise the temperature and pressure of the intake charge, eliminating the opportunity to reduce the compression work of the engine. Time was also the enemy of the Over-Expansion engine who's choked flow reduced the displaced volume on which the gases could work.

The theory of operation behind all these engine concepts suggested an improvement over conventional engines. The challenge they faced was to first overcome the additional friction, flow, heat losses, and knock propensity that their respective architectures generated before they could work towards that improvement. In these cases, that was too big a challenge to overcome. If departures are to be made from today's conventional engines, they will likely be simplistic in their architecture.

4.7 Suggestions for Future Work

One large disappointment was not being able to simulate the Six-Stroke Otto-Cycle engine. The Still Steam-Diesel engine is a historic example of an improvement in $\eta_{f,b}$ from a similar concept (steam processes ran in parallel instead of in series) and several theoretical investigations have suggested significant improvements. Either taking the coding step previously mentioned or utilizing some other software program to complete this analysis is suggested. Keep in mind that with two additional strokes per cycle, the FMEP will go up by 50% compared to a four-stroke cycle.

I also suggest further investigation into the idea presented in Section 2.2.3 where the potential benefits of true isochoric heat addition followed by fast piston motion could minimize the heat losses seen by Suzuki et al. while improving the realization of an ideal Otto-cycle. Care must be taken to understand and properly model FMEP, along with realizable instantaneous piston velocities.

Bibliography

[1] Douglas. The Museum of Retrotechnology. `http://www.douglas-self.com/MUSEUM/museum.htm`, April 2014.

[2] R. K. Raiput. *Thermal Engineering*. Laxim Publications, Bangalore, 5 edition, 2005.

[3] Capt. J. Aclund. (unknown title). Technical report, The Journal of the Society of Automotive Engineers, June 1920.

[4] Masatoshi Suzuki, Satoshi Iijima, Hayato Maehara, and Yasuo Moriyoshi. Effect of the ratio between connecting-rod length and crank radius on thermal efficiency. Technical Report 2006-32-0098, SAE International, 11 2006.

[5] Miin Jang Yan. Differential-stroke internal combustion engine. Patent US20130014713A1, USPTO, January 2013.

[6] Dulob AB. Dulob AB Vatne-Cycle and Thermocompression-Cycle. `http://www.dulob.com/`, 2014.

[7] Pete Lyons. Inside Bruce Crower's Six-Stroke Engine. *Auto Week*, February 2006. http://www.autoweek.com/article/20060227/free/302270007.

[8] James C. Conklin and James P. Szybist. A highly efficient six-stroke internal combustion engine cycle with water injection for in-cylinder exhaust heat recovery. *Energy by Elsevier*, 35:1658–1664, 2010.

[9] Bernard Johnson and Chris Edwards. Exploring the pathway to high efficiency IC engines through exergy analysis of heat transfer reduction. Technical Report 2013-01-0278, SAE International, January 2013.

[10] Gamma Technologies Inc. Various software manuals and tutorials. Version 7.3.

[11] Michael Grill, T. Billinger, and Michael Bargende. Quasi-dimensional modeling of spark ignition engine combustion with variable valve train. Technical Report 2006-01-1107, SAE International, January 2006.

[12] John B. Heywood. *Internal Combustion Engine Fundamentals*. McGraw-Hill, New York, 1988.

[13] Thomas Johansson, Patrick Borgqvist, Bengt Johansson, Per Tunestal, and Hans Aulin. HCCI heat release data for combustion simulation, based on results from a turbocharged multi cylinder engine. Technical Report 2010-01-1490, SAE International, May 2010.

[14] Gerald A. Szekely and Alex C. Alkidas. Combustion characteristics of a spray-guided direct-injection stratified-charge engine with a high-squish piston. Technical Report 2005-01-1937, SAE International, January 2005.

[15] Wikipedia. Darcy friction factor formulae. `http://en.wikipedia.org/wiki/Darcy_friction_factor_formulae`, May 2014.

[16] Janus A. Çengel. *Heat and Mass Transfer A Practical Approach*. McGraw-Hill, New York, 3 edition, 2007.

[17] Roy Ogink. Approximation of detailed-chemistry modeling by a simplified HCCI combustion model. Technical Report 2005-24-037, SAE International, September 2005.

A

Appendix

A.1 Model Verification

The following figures are generated to show how each concept cohered to the maximum exhaust gas temperature and burned residual limits.

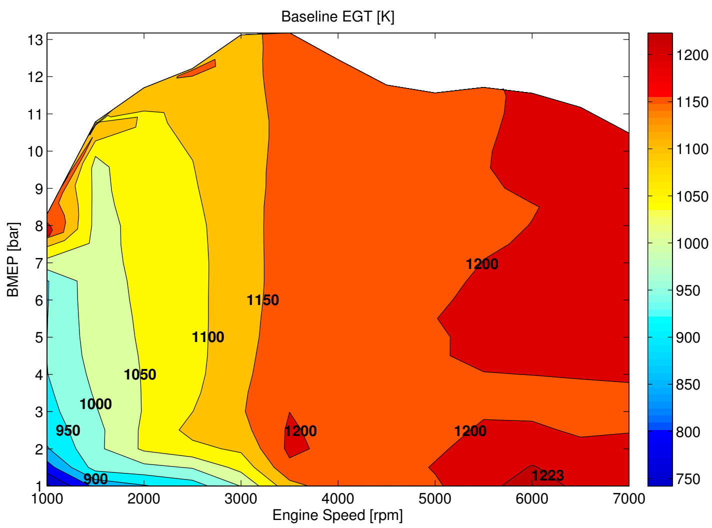

Figure A.1: Exhaust gas temperature in the exhaust port of the baseline engine throughout its entire load map. The criteria of less than 1223 K has been met at all but one load point, 1 *bar* at 6000 *rpm*. This load point is very uncommon in operation and is easily fixed with further simulation time.

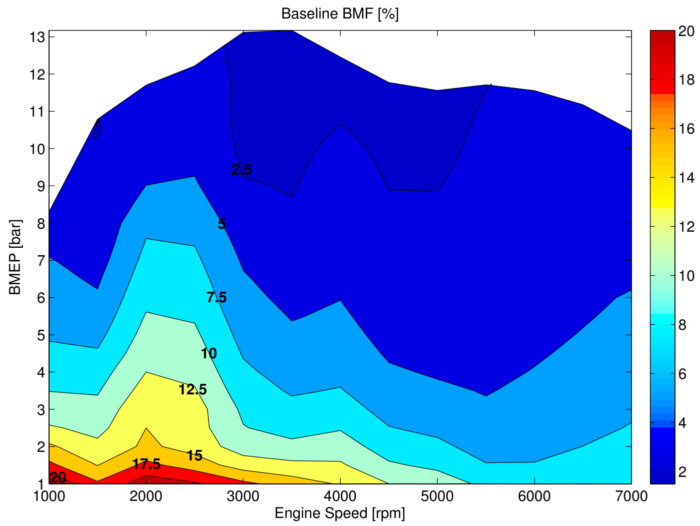

Figure A.2: Burned residuals trapped at the start of the next cycle of the baseline engine throughout its entire load map. The criteria of less than 25% has been met.

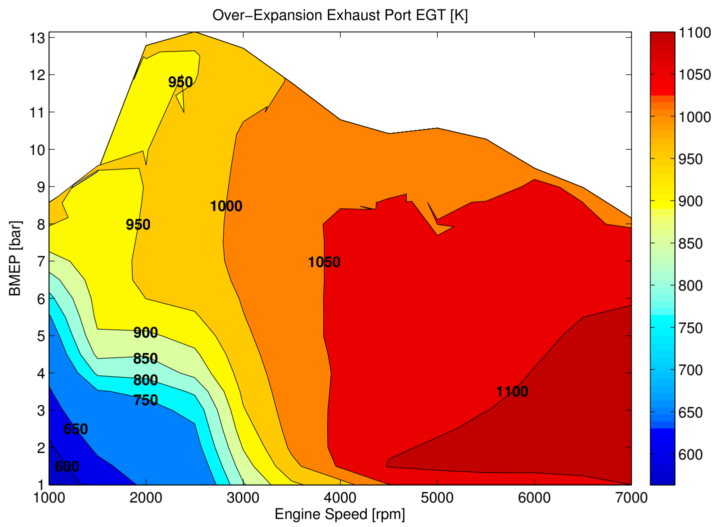

Figure A.3: Exhaust gas temperature in the exhaust port of the Over-Expansion engine throughout its entire load map. The criteria of less than 1223 K has been met without any fuel enrichment.

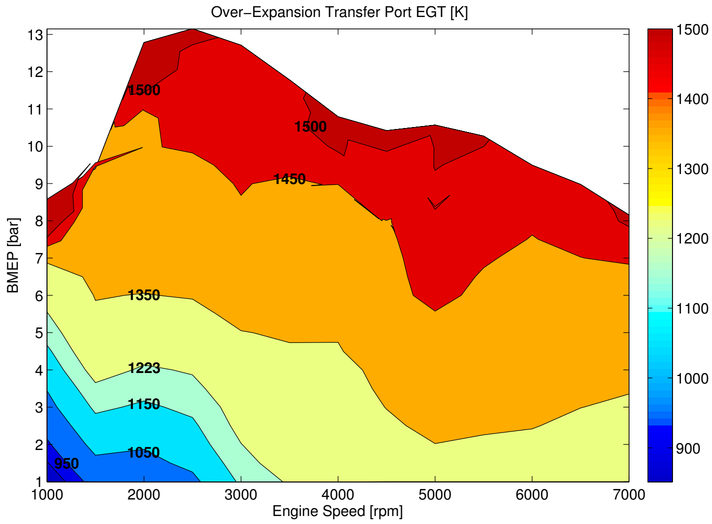

Figure A.4: Combustion gas temperature in the transfer port of the Over-Expansion engine throughout its entire load map. This does not come close to staying below 1223 K in the majority of the load map, but this was realized from the start since it is intended to transfer recently combusted gases.

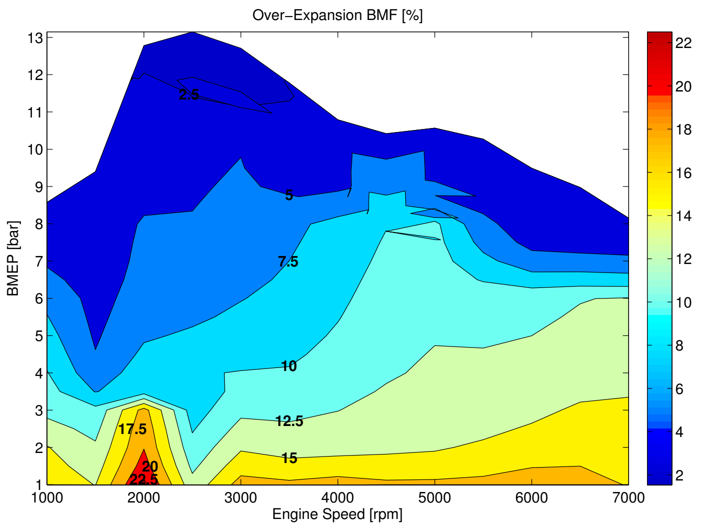

Figure A.5: Burned residuals trapped at the start of the next cycle in the firing cylinder of the Over-Expansion engine throughout its entire load map. The criteria of less than 25% has been met.

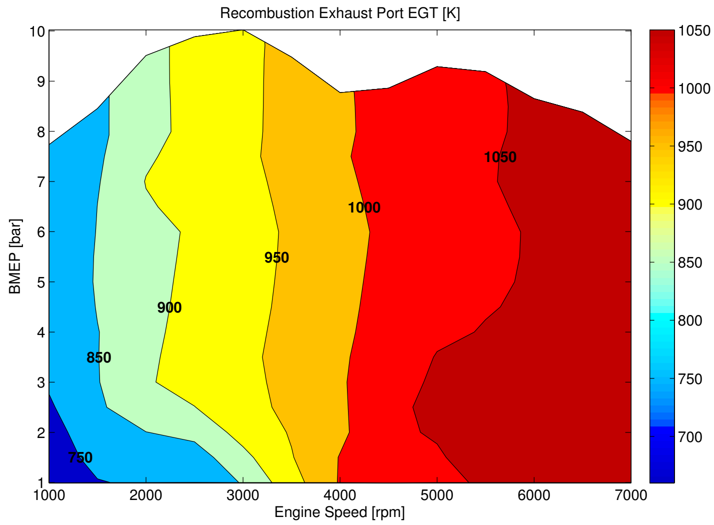

Figure A.6: Exhaust gas temperature in the exhaust port of the Recombustion engine throughout its entire load map. The criteria of less than 1223 K has been met without any fuel enrichment.

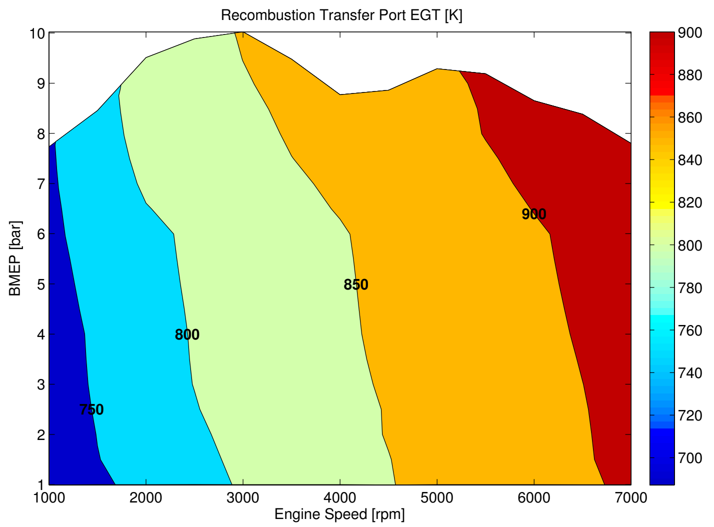

Figure A.7: Exhaust gas temperature in the transfer port of the Recombustion engine throughout its entire load map. The criteria of less than 1223 K has been met without any fuel enrichment.

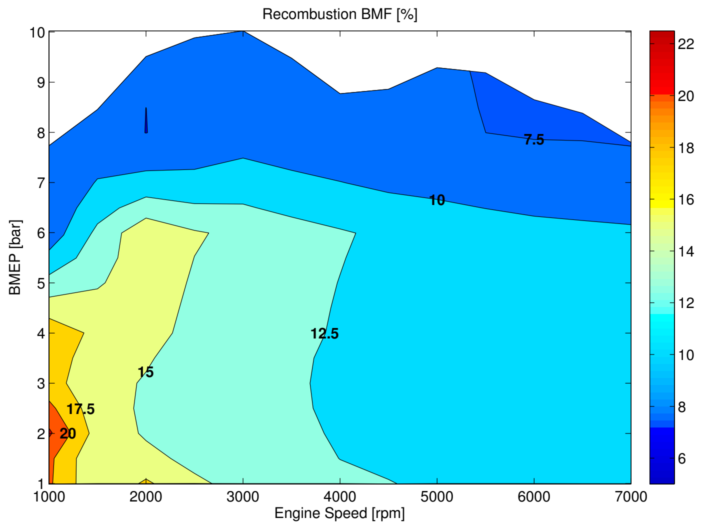

Figure A.8: Burned residuals trapped at the start of the next cycle in the stratified charge cylinder of the Recombustion engine throughout its entire load map. The criteria of less than 25% has been met.

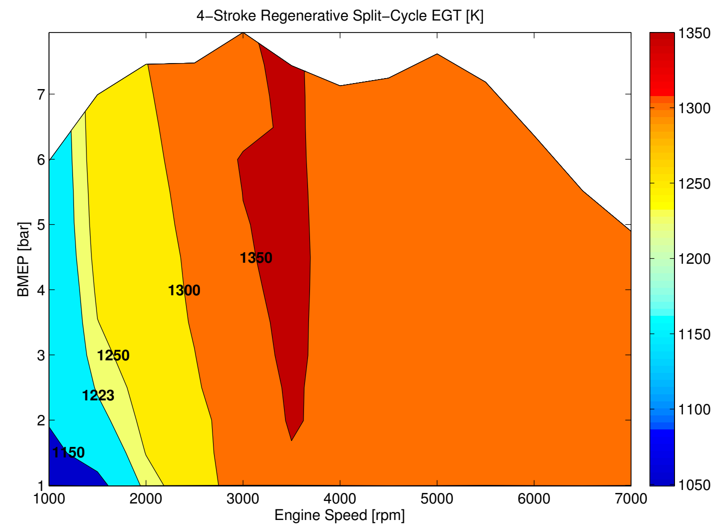

Figure A.9: Exhaust gas temperature for the 4-Stroke Regenerative Split-Cycle engine throughout its entire load map. The criteria of less than 1223 K has far been exceeded at nearly all load points. This is with fuel enrichment down to a minimum lambda of 0.82 (AFR of 12:1).

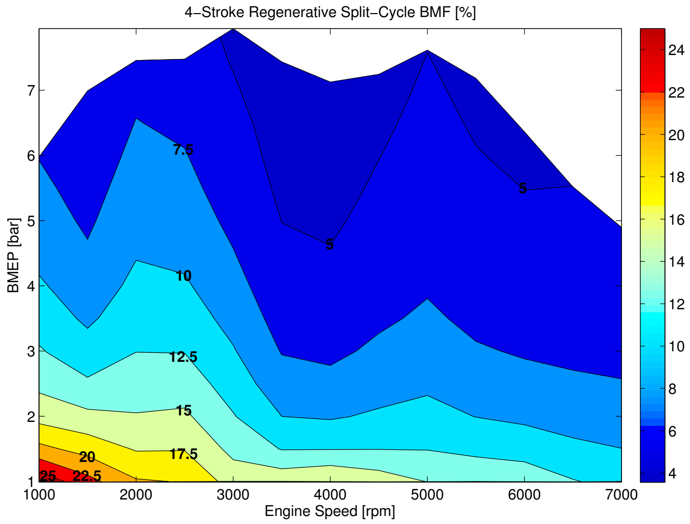

Figure A.10: Burned residuals trapped at the start of the next cycle in the firing cylinder of the 4-Stroke Regenerative Split-Cycle engine throughout its entire load map. The criteria of less than 25% has been met.